8735
NACA TN 2328

TECH LIBRARY KAFB, NM
0065074

NATIONAL ADVISORY COMMITTEE FOR AERONAUTICS

TECHNICAL NOTE 2328

METHOD FOR DETERMINING PRESSURE DROP OF MONATOMIC GASES FLOWING IN TURBULENT MOTION THROUGH CONSTANT-AREA PASSAGES WITH SIMULTANEOUS FRICTION AND HEAT ADDITION

By M. F. Valerino and R. B. Doyle

Lewis Flight Propulsion Laboratory
Cleveland, Ohio

Washington
April 1951

AFMDC
TECHNICAL LIBRARY
AFL 2811

TECH LIBRARY KAFB, NM

0065074

NATIONAL ADVISORY COMMITTEE FOR AERONAUTICS

TECHNICAL NOTE 2328

METHOD FOR DETERMINING PRESSURE DROP OF MONATOMIC GASES FLOWING IN TURBULENT MOTION THROUGH CONSTANT-AREA PASSAGES WITH SIMULTANEOUS FRICTION AND HEAT ADDITION

By M. F. Valerino and R. B. Doyle

SUMMARY

Charts are presented that enable convenient determination of the pressure drop sustained by monatomic gases (ratio of specific heats, 5/3) flowing at high subsonic speeds in a constant-area passage under the simultaneous influence of friction and heat addition.

Although the charts are constructed for determining pressure drops when heat is added at constant passage-wall temperature, pressure drops can be determined with good accuracy for other modes of heat addition through the use of an effective wall temperature in conjunction with these charts.

The effective wall temperature is given in terms of the passage dimensions, gas-flow conditions, and gas-temperature rise across the flow passage. The gas-temperature rise is related to the maximum passage-wall temperature for the cases of heat addition at constant wall temperature, constant rate of heat input along the passage length, and sine variation of heat input along the passage length.

INTRODUCTION

Many problems arise in aircraft heat-exchanger practice that involve the transfer of heat at high flux rates to a compressible fluid flowing at high speeds through constant-area flow passages. For example, in some recent heat-exchanger designs, the temperature differential between heat-exchanger wall and fluid approached values of the order of 1200° R and the fluid velocities approached the choke condition (Mach number, 1).

Methods have been developed for determining the pressure drop experienced in the passage of air through the radiator tubes of reciprocating engines (references 1 and 2). These methods contain simplifying assumptions that, although adequate over the range of

conditions encountered in aircraft radiators, cause appreciable error at the high airspeeds and heat-input rates considered herein.

In reference 3, the basic differential flow equation describing the pressure variations of a compressible fluid under the simultaneous action of friction and heat addition is numerically integrated for the specific case of air heated at constant passage-wall-temperature conditions. A closed-form solution of the basic differential flow equation is obtained in reference 4 for the special case of an exponential variation of fluid temperature with distance along the flow passage. In reference 5, the basic differential flow equation is formally integrated by use of a simplification that is shown to introduce little error in the description of the flow process; the integration results are presented for air in convenient chart form and are applicable for arbitrary heat-input distribution to the fluid along the flow passage.

Recently, interest has arisen in the use of monatomic gases as the working fluid in various aircraft closed cycles. The closed cycles involve the use of heat exchangers wherein heat is added to or subtracted from the monatomic gas. In the calculation of the performance of such closed cycles, a convenient means of determining the pressure and temperature changes of the monatomic gas flowing through the heat-exchanger passages is desirable.

In this report, which is the result of an investigation made at the NACA Lewis laboratory, charts are presented for calculating the pressure drop of monatomic gases (ratio of specific heats, 5/3) flowing in turbulent motion through smooth constant-area passages wherein heat is added to the fluid at constant passage-wall-temperature conditions. In the construction of the charts, the recent heat-transfer and fluid friction relations obtained in the experimental investigations of references 6 to 8 are used. Although the charts are for constant passage-wall-temperature conditions, it is shown that through the use of an effective passage-wall temperature the charts can be employed with good accuracy for other modes of heat input. The effective passage-wall temperature is taken as the constant passage-wall temperature that results in the same gas-temperature rise as obtained with the given mode of heat addition for the same gas-flow conditions and passage dimensions.

Plots are presented that relate the gas-temperature rise to the gas-flow conditions, maximum passage-wall temperature, and passage dimensions for the following modes of heat addition:

(a) Constant passage-wall temperature

(b) Constant rate of heat input along passage length

(c) Sine variation of heat input along passage length

Detailed examples are given that illustrate the use of the charts presented herein.

2100

SYMBOLS

The following symbols are used in this report:

A cross-sectional area of flow passage, (sq ft)

c_p specific heat of gas at constant pressure, (Btu/(lb)(°R))

D_e equivalent diameter of flow passage, which is equal to $4A/s$, (ft)

D_F drag force due to friction, (lb)

F friction factor, $\dfrac{-dp}{\frac{1}{2}\rho V^2 \frac{4dx}{D_e}}$

g mass conversion factor, 32.2 (lb/slug)

H heat added to gas in distance x per unit time, (Btu / sec)

H_t heat added to gas in total tube length L per unit time, (Btu)/(sec)

h heat-transfer coefficient between wall and gas, (Btu / (sec)(sq ft)(°R))

K constant

k thermal conductivity of gas, (Btu/(sec)(sq ft)(°R)/(ft))

L total tube length, (ft)

M Mach number

m mass flow of gas, (slugs/sec)

P total pressure, (lb/sq ft absolute)

p static pressure, (lb/sq ft absolute)

R gas constant, (ft-lb/(lb)(°R))

2100

s wetted perimeter, (ft)

T total temperature of gas, ($^{\circ}R$)

T_w temperature of passage walls, ($^{\circ}R$)

$T_{w,e}$ effective temperature of passage walls, ($^{\circ}R$)

$T_{w,max}$ maximum temperature of passage walls, ($^{\circ}R$)

t static temperature of gas, ($^{\circ}R$)

V velocity of gas in flow passage, (ft/sec)

x distance along flow passage (ft) as measured from station where T/T_w equals 0.20. This reference station may be a hypothetical one located in the forward extension of the given flow passage.

γ ratio of specific heats

ρ mass density of fluid, (slugs/cu ft)

μ absolute viscosity of fluid, (lb/ft-sec)

$\mu_{w,av}$ absolute viscosity of fluid evaluated at effective wall temperature of flow passage, (lb/ft-sec)

Subscripts:

en entrance of flow passage

ex exit of flow passage

w gas conditions evaluated at passage-wall temperature T_w

f gas conditions evaluated at average of fluid and passage-wall temperatures $\frac{T+T_w}{2}$

The following groupings of variables are involved:

M_p total-momentum parameter, $\frac{mV + pA}{m\sqrt{gRT}}$

2100

$\left(\frac{A\mu_w}{mgD_e}\right)^{0.2} \frac{x}{D_e}$ passage-distance parameter

$\left(\frac{A\mu_w}{mgD_e}\right)^{0.2} \frac{L}{D_e}$ passage-length parameter

$\frac{PA}{m\sqrt{gRT}}$ total-pressure parameter

$\frac{pA}{m\sqrt{gRT}}$ static-pressure parameter

ANALYSIS

The steady-flow process occurring within a constant-area heat-exchanger passage involves the simultaneous action of fluid friction and heat transfer. Analysis of this steady-flow process for the case of constant passage-wall temperature is presented herein. In addition, the applicability of and the method of conveniently using the analysis results for modes of heat input other than constant passage-wall temperature are determined.

Pressure drop and temperature rise for case of constant wall temperature. - One form of the differential momentum equation describing the one-dimensional steady-state motion of a compressible fluid in a constant-area passage under the combined influence of friction and heat transfer is

$$d(mV + pA) + dD_F = 0 \tag{1}$$

From the conservation of energy and mass equations and the perfect gas law, it is shown in reference 9 that the total-momentum parameter $\frac{mV + pA}{m\sqrt{gRT}}$ (herein denoted M_p) is uniquely related to each of the flow parameters M, $\frac{P}{p}$, $\frac{pA}{m\sqrt{gRT}}$, $\frac{T}{t}$, and $\frac{V}{\sqrt{gRT}}$ for any value of γ associated with the total temperature of the fluid. The equations relating

M_p to the aforementioned flow parameters for γ equal to a constant during the process are presented in convenient form in reference 5 (appendix B).

2100

It is evident, then, that knowledge of the variations of M_p and T during the flow process is sufficient to completely specify the variations of all the fluid-flow conditions (P, p, t, and V).

The variation of M_p during the flow process results from the variation of both $mV + pA$ and T. Differentiation of M_p with respect to these two variables for constant A and m gives

$$dM_p = \frac{d(mV+pA)}{m\sqrt{gRT}} - \frac{1}{2} M_p \frac{dT}{T} \tag{2}$$

The differential drag force dD_F is

$$dD_F = F \frac{1}{2} \rho V^2 A \frac{4\ dx}{D_e} \tag{3}$$

or, more conveniently,

$$dD_F = 2FmV \frac{dx}{D_e} \tag{4}$$

The variation of T is given by the differential relation equating the heat transferred from wall to fluid to the heat absorbed by the fluid

$$dH = mgc_p dT = hs(T_w - T)dx \tag{5}$$

The heat-transfer coefficient h and friction factor F are evaluated by use of equations (A1) and (A2) of appendix A. These equations are based on the recent data of references 6 to 8 obtained over a wide range of conditions, including Reynolds numbers up to 500,000, average tube-wall temperatures up to 2050° R, and heat-flux densities up to 150,000 Btu per hour per square foot. A comparison is presented in appendix A of pressure drops and temperature rises across the test tube as measured in a number of experimental runs and as calculated by means of equations (A1) and (A2).

2100

In view of the analogy between fluid friction and heat transfer given by equation (A4) of appendix A for flow through smooth-wall passages, equation (5) is rearranged and presented as

$$dT = 2\left(\frac{\frac{h}{c_p \rho g V}}{\frac{F}{2}}\right)(T_w - T)\, F\, \frac{dx}{D_e} \tag{6}$$

where, in reducing equation (5) to equation (6), the definition of D_e and the continuity equation $m = \rho A V$ are used.

From equations (1), (2), (4), and (6), the variation of M_p during the flow process is expressible as

$$dM_p = -\frac{V}{\sqrt{gRT}} \frac{dT}{\left(\frac{\frac{h}{c_p \rho g V}}{\frac{F}{2}}\right)(T_w - T)} - \frac{1}{2} M_p \frac{dT}{T} \tag{7}$$

The subsonic flow relation between M_p and $V/\sqrt{gRT}$ for constant γ is presented in appendix B of reference 5 as

$$\frac{V}{\sqrt{gRT}} = \frac{\gamma}{\gamma + 1}\left[M_p - \sqrt{M_p^2 - \frac{2(\gamma + 1)}{\gamma}}\right] \tag{8}$$

Eucken's rule between $c_p\mu/k$ and γ, as based on kinetic theory of gases, is

$$\frac{c_p \mu}{k} = \frac{4\gamma}{9\gamma - 5} \tag{9}$$

For T_w equal to a constant during the flow process,

$$d\left(\frac{T}{T_w}\right) = \frac{dT}{T_w} \tag{10}$$

For monatomic gases, γ equals the constant value of 5/3 (hence c_p is constant so that in equation (A4) $c_{p,w}/c_p = 1$). On the basis of equations (A4), (8), (9), and (10), equation (7) reduces to

$$\frac{dM_p}{d\left(\frac{T}{T_w}\right)} = \frac{\frac{5}{8}\left(\sqrt{M_p^2 - \frac{16}{5}} - M_p\right)}{\left(\frac{3}{2}\right)^{0.6}\left(1 - \frac{T}{T_w}\right)} - \frac{M_p}{2\left(\frac{T}{T_w}\right)} \tag{11}$$

2100

The variation of M_p is uniquely related to the variation of T/T_w during the flow process by equation (11).

In the integration of equation (11), the lower integration limit for T/T_w is arbitrarily taken constant as 0.20, whereas the lower integration limit for M_p is assigned about 35 different values that cover the range of M_p corresponding to Mach numbers from 0.10 to 0.90. The integration is numerically performed to values of M_p corresponding to choke (Mach number, 1) or to an arbitrarily assigned value of T/T_w equal to 0.92, whichever is attained first in the integration.

By equation (11), M_p is shown to be explicitly independent of the position variable x; hence each corresponding pair of values of T/T_w and M_p obtained in an integration performed for a given set of lower integration limits can be considered as a possible entrance condition of a flow passage. It is evident, then, that although the lower integration limit for T/T_w is 0.20, the integration results are applicable for any values of T/T_w at the passage entrance greater than 0.20.

From the integration results and the relations between M_p and $PA/m\sqrt{gRT}$ (or $pA/m\sqrt{gRT}$) presented in reference 5, the variation between $PA/m\sqrt{gRT}$ (or $pA/m\sqrt{gRT}$) and T/T_w is obtained. The results are presented in figures 1 and 2 as plots of $PA/m\sqrt{gRT}$ and $pA/m\sqrt{gRT}$, respectively, against T/T_w. Included in figures 1 and 2 is a scale giving the Mach number values M corresponding to the values of $PA/m\sqrt{gRT}$ and $pA/m\sqrt{gRT}$.

The foregoing analysis relates the variation in the fluid-flow conditions to the T/T_w variation obtained during the process. In order to obtain the fluid-flow conditions as a function of position along a flow passage, it is therefore necessary to know how T/T_w varies with distance along the flow passage. The following analysis provides the required relation between T/T_w and x:

2100

Substitution of equation (A1) into equation (5) and use of the continuity relation $m = \rho AV$ and the definition of D_e result in

$$dT = \left[0.092 \frac{c_{p,w}}{c_p}\left(\frac{k_w}{c_{p,w}\mu_w}\right)^{0.6}\right]\left(\frac{T}{T_w}\right)^{0.8}(T_w - T)\left(\frac{A\mu_w}{mgD_e}\right)^{0.2}\frac{dx}{D_e} \tag{12}$$

From equations (9) and (10), for monatomic gases ($\gamma = 5/3$, $c_{p,w}/c_p = 1$)

$$\frac{d\left(\frac{T}{T_w}\right)}{\left(\frac{T}{T_w}\right)^{0.8}\left(1 - \frac{T}{T_w}\right)} = 0.1174\left(\frac{A\mu_w}{mgD_e}\right)^{0.2}\frac{dx}{D_e} \tag{13}$$

Integration of equation (13) gives

$$0.1174\left(\frac{A\mu_w}{mgD_e}\right)^{0.2}\frac{x}{D_e}\Bigg]_{x_0}^{x} = \left\{\log_e \frac{(Z^2 + 1.6180\,Z + 1)^{0.809}}{\left[(1-Z)Z^2 - 0.6180\,Z + 1)\right]^{0.309}} + 1.9021\tan^{-1}\left(\frac{2Z - 0.6180}{1.9021}\right) + 1.1756\tan^{-1}\left(\frac{2Z + 1.6180}{1.1756}\right)\right\}\Bigg]_{Z_0}^{Z} \tag{14}$$

where $Z = (T/T_w)^{1/5}$.

The lower integration limits are arbitrarily taken as $x_0 = 0$ and $Z_0 = (0.20)^{1/5}$. These limits are consistent with those taken in integration of equation (11).

A plot of equation (14) is presented as figure 3 wherein T/T_w is the ordinate and $\left(\frac{A\mu_w}{mgD_e}\right)^{0.2}\frac{x}{D_e}$ is the abscissa.

Applicability of figures 1 and 2 for other modes of heat input. - Although figures 1 and 2 are for the case of constant wall temperature, they can be applied to other modes of heat input through the use of an effective wall temperature $T_{w,e}$, as shown herein. The effective wall

temperature is defined as the constant wall temperature resulting in the same temperature rise of the gas for the specified gas-flow conditions and passage geometry as that obtained with the given mode of heat input. Hence, by definition, $T_{w,e}$ is the same as T_w plotted in figure 3. Inasmuch as figure 3 is not in convenient form for determining T_w (or $T_{w,e}$), a replot of figure 3 is presented as figure 4 where T_{ex}/T_{en} is plotted against $\left(\frac{A\mu_{w,av}}{mgD_e}\right)^{0.2} \frac{L}{D_e}$ with $T_{en}/T_{w,e}$ as the curve parameter.

The following table is presented to show the validity of using the effective wall temperature in conjunction with figures 1 and 2 to determine pressure drop for modes of heat input other than constant wall temperature. Two modes of heat input are considered herein; namely, constant rate of heat input, and sine variation of heat input along the passage length, both of which represent a radical departure from the case of constant passage-wall temperature. The table gives a comparison, for these two modes of heat input, of the pressure drop obtained by use of figures 1 and 2 in conjunction with the effective wall temperature and the pressure drop obtained by integration of the flow differential equation for the particular mode of heat input. The comparison is made over a range of flow Mach number for T_{ex}/T_{en} equal to 2.0.

M_{en}	M_{ex}	Type of heat distribution	$\left(\frac{\Delta P}{P_{en}}\right)_{calc}$	$\left(\frac{\Delta P}{P_{en}}\right)_{chart}$	Difference (percent)
0.207	0.348	Constant rate of heat input	0.124	0.125	0.8
.240	.458	Constant rate of heat input	.181	.183	1.1
.267	.600	Constant rate of heat input	.244	.250	2.5
.280	.710	Constant rate of heat input	.279	.285	2.2
.207	.348	Sine variation with distance	.127	.125	1.6
.240	.458	Sine variation with distance	.183	.183	0
.267	.600	Sine variation with distance	.250	.250	0
.280	.702	Sine variation with distance	.288	.285	1.1

2100

The agreement indicated in the foregoing table is of the same order of magnitude as the accuracy with which figures 1 and 2 can be read. It is evident, then, that figures 1 and 2 can be used with good accuracy to determine pressure drops in flow passages where the heat-input distribution radically departs from the constant passage-wall condition by assuming the heat input to the gas to be at constant passage-wall temperature with T_w equal to $T_{w,e}$.

Effective wall temperature for two special modes of heat input. - In appendix B, an analysis is presented that relates the temperature rise of the gas to the passage dimensions, gas-flow conditions, and maximum passage-wall temperature for the cases of constant rate of heat input and sine variation of heat input along the passage length. In figures 5 and 6, which give the analysis results, $T_{en}/T_{w,max}$ is plotted against $\left(\frac{A\mu_{w,av}}{mgD_e}\right)^{0.2} \frac{L}{D_e}$ with T_{ex}/T_{en} as the curve parameter. As demonstrated later in Example III, figures 5 and 6 used in conjunction with figure 4 enable convenient determination of $T_{w,e}/T_{w,max}$ for the two modes of heat input treated herein.

DESCRIPTION OF CHARTS

In figures 1 and 2, the ratio of gas total temperature to passage-wall temperature T/T_w for the case of constant passage-wall temperature along the passage length is plotted against the total- and static-pressure parameters $PA/m\sqrt{gRT}$ and $pA/m\sqrt{gRT}$. (In figs. 1 and 2 the lines are alternately dashed and solid for convenience in reading.) A scale of Mach number to give the values of M corresponding to those of $PA/m\sqrt{gRT}$ and $pA/m\sqrt{gRT}$ is included. The path described by any of the curves in figures 1 and 2, going from right to left, describes the variation of $PA/m\sqrt{gRT}$ and $pA/m\sqrt{gRT}$ (or M) with T/T_w in a constant-area flow passage where T_w is constant. Hence, if T/T_w and M (or $PA/m\sqrt{gRT}$, or $pA/m\sqrt{gRT}$) at the flow-passage entrance are known, the point on figure 1 or 2 representing the gas conditions at the passage entrance is fixed. The curve on which this point lies (in fig. 1 or 2) is the line describing the flow variations along the passage. If T/T_w at the passage exit is known (T_{ex}/T_w will be greater than T_{en}/T_w because of heating), proceed along the curve to where the curve intersects the ordinate value $T/T_w = T_{ex}/T_w$. This point represents the flow conditions at the passage exit and hence gives the

values of M_{ex} and $(PA/m\sqrt{gRT})_{ex}$ (or $(pA/m\sqrt{gRT})_{ex}$). This procedure is later illustrated in step-by-step fashion in Example I.

2100

In figure 3, the ratio of the gas total temperature to the passage-wall temperature T/T_w is plotted against the distance parameter $\left(\frac{A\mu_w}{mgD_e}\right)^{0.2}\frac{x}{D_e}$ for constant passage-wall temperature along the passage length. If T/T_w at the passage entrance (that is, T_{en}/T_w) is known and is equal to or greater than 0.20, figure 3 first gives the distance parameter for the passage entrance $\left(\text{that is, } \left(\frac{A\mu_w}{mgD_e}\right)^{0.2}\frac{x_{en}}{D_e}\right)$. Note that x_{en} is the distance between the passage entrance and a station in the hypothetical forward extension of the passage characterized by $T/T_w = 0.20$. The distance parameter for the passage exit is then calculated as $\left(\frac{A\mu_w}{mgD_e}\right)^{0.2}\frac{x_{en} + L}{D_e}$ where L is the passage length. Figure 3 is then finally used to determine the T/T_w corresponding to the distance parameter for the passage exit; this value of T/T_w is the required value of T_{en}/T_w. This procedure is later illustrated in step-by-step fashion in Example II.

In figure 4, which is a replot of figure 3 in a form more convenient for determining T_w, is a plot of the ratio of the exit to entrance total temperature of the gas T_{ex}/T_{en} against the passage-length parameter $\left(\frac{A\mu_{w,av}}{mgD_e}\right)^{0.2}\frac{L}{D_e}$ for various ratios of entrance total temperature of the gas to effective wall temperature $T_{en}/T_{w,e}$. As a result of the definition of $T_{w,e}$, figure 4 is applicable for any mode of heat input. The use of figure 4 in conjunction with figures 1 and 2 to determine the pressure drop of a monatomic gas flowing in a heated passage for modes of heat input other than at constant passage-wall temperature is briefly outlined as follows:

(a) For the given heat-input distribution along the passage length, the temperature rise of the gas is determined from the heat-balance relation

$$T_{ex} - T_{en} = \frac{1}{mgc_p}\int_{x_{en}}^{x_{ex}} \frac{dH}{dx}\,dx$$

where the integration is numerically performed for complicated heat-input distributions.

2100

(b) The value of $T_{w,e}$ can be obtained from the known gas-flow conditions, passage dimensions, and entrance and exit total temperatures of the gas by use of figure 4.

(c) Figures 1 and 2 are then used by treating the problem as one for constant wall-temperature conditions with $T_w = T_{w,e}$.

Steps (b) and (c) of the foregoing procedure are illustrated later in detail in Example III.

The relations of the gas total-temperature rise in a flow passage to the flow conditions, passage dimensions, and maximum passage-wall temperature are given in figures 5 and 6. In figure 5, which is for the case of constant rate of heat input along the passage length, the ratio of the fluid-entrance temperature to the maximum passage-wall temperature $T_{en}/T_{w,max}$ is plotted against the passage-length parameter $\left(\frac{A\mu_{w,av}}{mgD_e}\right)^{0.2} \frac{L}{D_e}$ for various ratios of the exit to entrance total temperature of the gas T_{ex}/T_{en}. A similar plot for the case of sine variation of heat input along the passage length is given in figure 6. The use of figures 5 and 6 is described later in detail in Example III.

For convenience, a plot of the absolute viscosity of helium against temperature, as given by reference 10, is presented in figure 7.

EXAMPLES ILLUSTRATING USE OF CHARTS

Example I

The use of figures 1 and 2 is illustrated for pressure-drop determination with heat input at constant passage-wall temperature.

A monatomic gas is heated during flow through a constant-area smooth-wall passage. The passage walls are at a constant temperature throughout their length. The flow and heating conditions are as follows:

(1) T_{en}/T_w 0.30
(2) T_{ex}/T_w 0.80
(3) M_{en} 0.20

Determine: M_{ex} and P_{ex}/P_{en}

(4) The point in figure 1 representing the flow conditions at the passage entrance has abscissa (top scale) = 0.20 (item (3)) and ordinate = 0.30 (item (1)). This point is designated point a in figure 8, which is a small-scale reproduction of figure 1 and is presented for illustrative purposes. 2100

(5) For point a, the lower abscissa scale reads

$$\frac{P_{en}A}{m\sqrt{gRT_{en}}} = 3.974$$

(6) From point a, follow the flow-path lines up to the point where $T/T_w = 0.80$ (item (2)) in the manner illustrated in figure 8. The point where $T/T_w = 0.80$ obtained by this procedure is designated point b in figure 8 and represents the flow conditions at the passage exit.

(7) For point b, the lower abscissa scale reads

$$\frac{P_{ex}A}{m\sqrt{gRT_{ex}}} = 1.846$$

and the upper abscissa scale reads

$$M_{ex} = 0.49$$

(8) For T_w = a constant, from items (1), (2), (5), and (7),

$$\frac{P_{ex}}{P_{en}} = \frac{\dfrac{P_{ex}A}{m\sqrt{gRT_{ex}}}}{\dfrac{P_{en}A}{m\sqrt{gRT_{en}}}}\sqrt{\frac{\dfrac{T_{ex}}{T_w}}{\dfrac{T_{en}}{T_w}}} = \frac{1.846}{3.974}\sqrt{\frac{0.80}{0.30}} = 0.759$$

The procedure for determining the static-pressure ratio p_{ex}/p_{en} is the same as that illustrated for the total-pressure ratio P_{ex}/P_{en} except that figure 2 is used instead of figure 1.

2100

Example II

The use of figure 3 in conjunction with figures 1 and 2 is illustrated for pressure-drop determination with heat input at constant passage-wall temperature.

The flow and heating conditions are as follows:

(1)	T_{en}, °R	500
(2)	T_w, °R	1667
(3)	P_{en}, lb/sq ft	3000
(4)	D_e, ft	0.02
(5)	L, ft	1.98
(6)	M_{en}	0.20
(7)	Helium gas (R = 386.4)	

Determine: T_{ex} and P_{ex}/P_{en}

(8) As in Example I, from figure 1 and item (6),

$$\frac{P_{en}A}{m\sqrt{gRT_{en}}} = 3.974$$

(9) From items (1), (3), (7), and (8),

$$\frac{m}{A} = \frac{m\sqrt{gRT_{en}}}{P_{en}A}\,\frac{P_{en}}{\sqrt{gRT_{en}}}$$

$$= \frac{1}{3.974}\,\frac{3000}{\sqrt{32.2 \times 386.4 \times 500}}$$

$$= 0.303 \text{ (slugs/sq ft-sec)}$$

(10) From figure 7 and items (2) and (7),

$$\mu_w = 28.1 \times 10^{-6} \text{ (lb/ft-sec)}$$

(11) From items (4), (5), (9), and (10),

$$\left(\frac{A\mu_w}{mgD_e}\right)^{0.2} \frac{L}{D_e} = \left(\frac{28.1 \times 10^{-6}}{0.303 \times 32.2 \times 0.02}\right)^{0.2} \frac{1.98}{0.02} = 16.87$$

2100

(12) From items (1) and (2),

$$\frac{T_{en}}{T_w} = \frac{500}{1667} = 0.30$$

(13) From figure 3 and item (12),

$$\left(\frac{A\mu_w}{mgD_e}\right)^{0.2} \frac{x_{en}}{D_e} = 3.45$$

which is the distance parameter between a hypothetical station in the forward extension of the flow passage, as characterized by $T/T_w = 0.20$, and the passage entrance (where $T/T_w = 0.30$ in this case).

(14) The distance parameter between the hypothetical station characterized by $T/T_w = 0.20$ and the passage exit is given simply as the sum of items (11) and (13):

$$\left(\frac{A\mu_w}{mgD_e}\right)^{0.2} \frac{x_{ex}}{D_e} = 3.45 + 16.87 = 20.32$$

(15) From figure 3 and item (14),

$$\frac{T_{ex}}{T_w} = 0.80$$

(16) In order to determine M_{ex} and P_{ex}/P_{en}, proceed as in Example I. Inasmuch as M_{en}, T_{en}/T_w, and T_{ex}/T_w are the same as in Example I, the required values of M_{ex} and P_{ex}/P_{en} are the same as determined in Example I.

2100

Example III

The use of figures 4 and 5 to determine effective wall temperature and the application of figures 1 and 2 to the case of constant rate of heat input along the flow-passage length are illustrated.

The heat input to helium flowing in a constant-area smooth-wall passage is assumed to be at a constant rate along the passage length. The flow and heating conditions are as follows:

(1) T_{en}, °R 500

(2) $T_{w,max}$, °R 1900

(3) $\left(\frac{A\mu_{w,av}}{mgD_e}\right)^{0.2} \frac{L}{D_e}$ 16.80

(4) M_{en} 0.20

Determine: $T_{w,e}$, $T_{en}/T_{w,e}$, $T_{ex}/T_{w,e}$, M_{ex}, and P_{ex}/P_{en}

(5) From items (1) and (2),

$$\frac{T_{en}}{T_{w,max}} = \frac{500}{1900} = 0.263$$

(6) From figure 5 and items (3) and (5),

$$\frac{T_{ex}}{T_{en}} = 2.67$$

(7) From figure 4 and items (3) and (6),

$$\frac{T_{en}}{T_{w,e}} = 0.30$$

so that from item (1),

$$T_{w,e} = 1667 \ (^{\circ}R)$$

(8) From items (6) and (7),

$$\frac{T_{ex}}{T_{w,e}} = \frac{T_{en}}{T_{w,e}} \frac{T_{ex}}{T_{en}} = 0.30 \times 2.667 = 0.80$$

2100

(9) Figures (1) and (2) are used to determine M_{ex}, P_{ex}/P_{en}, and p_{ex}/p_{en} in the same manner as illustrated in Example I except that $T/T_{w,e}$ is used in place of T/T_w. (Note that in example I, T_w is a constant, whereas in this example T_w is a function of distance along the passage. However, $T_{w,e}$ is a constant by definition and herein corresponds to the constant T_w of Example I.)

For the case of sine variation of heat input, the same procedure as outlined in this example is followed except that figure 6 is used in place of figure 5.

Example IV

The determination of the mass flow of gas through a constant-area heated flow passage corresponding to a specified pressure drop is illustrated.

The flow and heating conditions are as follows:

(1) p_{en}, lb/sq ft 4000
(2) p_{ex}, lb/sq ft 3000
(3) $T_{en}/T_{w,e}$ 0.30
(4) $T_{ex}/T_{w,e}$ 0.80
(5) T_{en}, °R 500

Determine: m/A

(6) From items (1) to (4), the ratio of the static-pressure parameter at the exit and the entrance of the passage must be

$$\frac{\dfrac{p_{ex}A}{m\sqrt{gRT_{ex}}}}{\dfrac{p_{en}A}{m\sqrt{gRT_{en}}}} = \frac{p_{ex}}{p_{en}}\sqrt{\frac{\dfrac{T_{en}}{T_{w,e}}}{\dfrac{T_{ex}}{T_{w,e}}}} = \frac{3000}{4000}\sqrt{\frac{0.30}{0.80}} = 0.459$$

2100

(7) The problem is to determine the value of $\frac{p_{en}A}{m\sqrt{gRT_{en}}}$ such that

$$\text{(a)}\quad \frac{\dfrac{p_{ex}A}{m\sqrt{gRT_{ex}}}}{\dfrac{p_{en}A}{m\sqrt{gRT_{en}}}} = 0.459 \quad \text{(item (6))}$$

$$\text{(b)}\quad \frac{T_{ex}}{T_{w,e}} = 0.80 \quad \text{(item (4))}$$

The procedure used is illustrated in figure 9, which is a small-scale reproduction of figure 2 presented for illustrative purposes.

(8) Assume $\frac{p_{en}A}{m\sqrt{gRT_{en}}} = 3.50$, point a in figure 9. From item 7(a), it is necessary that $\frac{p_{ex}A}{m\sqrt{gRT_{ex}}} = 0.459 \times 3.50 = 1.607$. Hence, follow the flow-path line in the manner illustrated up to the point where $\frac{p_{ex}A}{m\sqrt{gRT_{ex}}} = 1.607$, point a_1 in figure 9.

(9) Assume $\frac{p_{en}A}{m\sqrt{gRT_{en}}} = 4.00$ and repeat the procedure outlined in item (8). Designate the point representing the entrance conditions point b and the corresponding point representing the exit conditions as point b_1 in figure 9.

(10) Repeat the procedure for an assumed value of $\frac{p_{en}A}{m\sqrt{gRT_{en}}} = 4.50$, designating the points in figure 9 points c and c_1.

(11) Draw a curve through the points a_1, b_1, and c_1 and one through the points a, b, and c. The point on curve $a_1b_1c_1$ with ordinate value $T/T_w = 0.80$ represents the conditions at the passage exit consistent with the given conditions (items (1) through (4)). This point is designated point d_1 in figure 9.

(12) The corresponding condition at the passage entrance is obtained by following the flow-path lines back from point d_1 to intersect the curve abc. This intersection is designated point d in figure 9. Point d gives the required value of $\frac{p_{en}A}{m\sqrt{gRT_{en}}}$ satisfying the conditions given in items (7(a)) and (7(b)). 2100

(13) The lower abscissa value for point d is

$$\frac{p_{en}A}{m\sqrt{gRT_{en}}} = 4.282$$

(14) Hence from items (1), (5), and (13) for R = 386.4 (helium)

$$\frac{m}{A} = \frac{m\sqrt{gRT_{en}}}{p_{en}A}\,\frac{p_{en}}{\sqrt{gRT_{en}}}$$

$$\frac{m}{A} = \frac{1}{4.282}\,\frac{4000}{\sqrt{32.2 \times 386.4 \times 500}} = 0.374 \text{ (slugs/sec-sq ft)}$$

Lewis Flight Propulsion Laboratory,
National Advisory Committee for Aeronautics,
Cleveland, Ohio, November 3, 1950.

2100

APPENDIX A

HEAT-TRANSFER AND FLUID-FRICTION RELATIONS

Some recent data available on heat-transfer coefficient and friction factor for fluid flow through smooth passages are given by the extensive experimental investigations of references 6 and 7. These data were obtained with air flowing through an electrically heated Inconel tube with an inside diameter of 0.4 inch and a length of 24 inches for various types of tube-entrance section. The range of conditions investigated included Reynolds numbers up to 500,000, average tube-wall temperatures up to 2050° R, and heat flux densities up to 150,000 Btu per hour per square foot. Based on the correlation results of references 6 to 8 obtained for the entire range of surface temperatures and for Reynolds numbers above 10,000, the following equation for local heat-transfer coefficient h is used in the analysis of this report:

$$\frac{hD_e}{k_w} = 0.023 \left(\frac{\rho V g D_e}{\mu_w}\right)^{0.8} \left(\frac{c_{p,w}\mu_w}{k_w}\right)^{0.4} \left(\frac{T}{T_w}\right)^{0.8} \tag{A1}$$

A comparison, for a number of experimental runs, between experimental and calculated temperature-rise values (using equation (A1)), gave agreement within 10 percent.

Several equations for correlating friction factor, none of which is completely satisfactory, were used in references 7 and 8; nevertheless, improved correlation over that given by the conventional correlation method was obtained. The two more satisfactory correlation equations are given by

$$F = 0.046 \left(\frac{\mu_w}{\rho_w V g D_e}\right)^{0.2} \left(\frac{\rho_w}{\rho}\right) \tag{A2}$$

$$F = 0.046 \left(\frac{\mu_w}{\rho_w V g D_e}\right)^{0.2} \left(\frac{\rho_f}{\rho}\right) \tag{A3}$$

The validity of using equation (A2) or (A3) for calculating local friction factors is measured by how accurately pressure-drop predictions can be made through the use of these equations. Comparison is made herein between calculated and measured pressure variations along the test passage of references 7 and 8 for a number of experimental runs conducted at high

heat inputs to the fluid at both low- and high-flow Mach numbers. The calculated pressure variations were determined using both equations (A2) and (A3) in order to determine which of these two equations results in best agreement with the experimental data. The test conditions of the experimental runs and the comparison results are tabulated as follows:

2100

M_{en}	M_{ex}	$T_{w,av}$	T_{en}	T_{ex}	$\Delta p/p_{en}$		
					Experimental	Calculated (equation (A2))	Calculated (equation (A3))
0.410	0.722	1072	554	753	0.361	0.348	0.418
.400	.770	1273	530	798	.346	.326	.392
.358	.732	1677	525	917	.381	.350	.433
.411	.836	1196	543	781	.352	.326	.392
.172	.234	1246	552	904	.063	.058	.063
.374	.839	1679	528	903	.383	.352	.425
.358	.632	1272	529	812	.316	.269	.317

Inasmuch as in the experiments the heat was added to the fluid at essentially constant rate along the passage, the fluid temperature was taken to vary linearly across the passage. In order to reduce entrance effects, the fluid conditions to start the calculations were taken as those existing in the test passage at a distance of 4 inches (10 diam.) downstream of the entrance.

The foregoing table indicates that equation (A2) gives better agreement with the experimental data at the high Mach numbers; at the low Mach numbers, equation (A3) gives better agreement.

For the analysis presented in this report, equation (A2) is chosen to represent the friction process.

From equations (A1) and (A2),

$$\frac{\dfrac{h}{c_p \rho V g}}{\dfrac{F}{2}} = \left(\frac{c_{p,w}}{c_p}\right)\left(\frac{c_{p,w}\mu_w}{k_w}\right)^{-0.6} \tag{A4}$$

2100

APPENDIX B

RELATION BETWEEN GAS-TEMPERATURE RISE AND MAXIMUM WALL TEMPERATURE FOR CONSTANT HEAT FLUX ALONG PASSAGE AND SINE HEAT-INPUT VARIATION ALONG PASSAGE

Relations are derived herein that will permit determination of the temperature rise of the gas in terms of the passage dimensions, gas-flow conditions, and maximum passage-wall temperature for the cases of constant heat flux along the passage and sine heat-input variation along the passage.

Constant heat flux along passage. - The case of constant heat flux is characterized by

$$\frac{dH}{dx} = \frac{H_t}{L} \tag{B1}$$

From equations (5) and (B1), the continuity equation $m = \rho AV$, and the definition of D_e,

$$\frac{H_t}{(L/D_e)mgc_pT} = \frac{4h}{\rho Vgc_p}\left(\frac{T_w}{T} - 1\right) \tag{B2}$$

Substitution of equation (A1) in equation (B2) results in

$$\frac{H_t}{(L/D_e)mgc_pT} = 0.092\left(\frac{k_w}{c_{p,w}\mu_w}\right)^{0.6}\left(\frac{A\mu_w}{mgD_e}\right)^{0.2}\left(\frac{T}{T_w}\right)^{0.8}\left(\frac{T_w}{T} - 1\right) \tag{B3}$$

wherein, for monatomic gases, $c_{p,w}/c_p = 1$.

The total amount of heat added to a fluid in the over-all passage length L can be given as

$$H_t = mgc_p\,(T_{ex}-T_{en}) \tag{B4}$$

At any flow cross section of the passage, equation (B3) is applicable. When applied to the exit of the passage, T in equation (B3) is replaced by T_{ex} and subscript w is replaced by subscript w,ex. Hence, from equations (9), (B3), and (B4) for $\gamma = 5/3$,

2100

$$\left(\frac{A\mu_{w,ex}}{mgD_e}\right)^{0.2} \frac{L}{D_e} = \frac{1 - \frac{T_{en}}{T_{ex}}}{0.1174 \left(\frac{T_{en}}{T_{w,ex}}\right)^{0.8} \left(\frac{T_{ex}}{T_{en}}\right)^{0.8} \left(\frac{T_{w,ex}}{T_{en}} \frac{T_{en}}{T_{ex}} - 1\right)} \tag{B5}$$

For the case of constant heat flux along the passage, the exit passage-wall temperature $T_{w,ex}$ is the maximum wall temperature $T_{w,max}$. A plot of equation (B5) is presented as figure 5. Because $(\mu_w)^{0.2}$ varies only slightly with temperature, $\mu_{w,ex}$ is replaced by $\mu_{w,av}$ in figure 5 in order to permit convenient use of figure 5 in conjunction with figure 4 for determining effective wall temperature.

Sine heat-input variation along passage. - For the case of sine heat-input variation along the passage,

$$dH = K \sin \frac{\pi x}{L} dx \tag{B6}$$

Combination of the relation $dH = mgc_p dT$ (equation (5)) and equation (B6) and integration result in

$$\frac{T}{T_{en}} = 1 + \frac{KL}{\pi mgc_p T_{en}} \left(1 - \cos \frac{\pi x}{L}\right) \tag{B7}$$

In equation (B7), when $x = L$, $T = T_{ex}$ so that

$$\frac{KL}{\pi mgc_p T_{en}} = \frac{1}{2}\left(\frac{T_{ex}}{T_{en}} - 1\right) \tag{B8}$$

Combination of the relation $dH = hs(T_w - T)dx$ (equation (5)) and equation (B6) and substitution for h from equation (A1) give

2100

$$\left(\frac{T}{T_w}\right)^{0.8}\left(\frac{T_w}{T} - 1\right) = \frac{\sin\frac{\pi x}{L}}{\frac{YT}{K}} \tag{B9}$$

where

$$Y = 0.023\ c_{p,w}\mu_w^{0.2}\left(\frac{k_w}{c_{p,w}\mu_w}\right)^{0.6}\left(\frac{mgD_e}{A}\right)^{0.8}\frac{s}{D_e} \tag{B10}$$

The condition of maximum wall temperature is given by $dT_w/dx = 0$ Differentiating equation (B9) with respect to x and setting $dT_w/dx = 0$ give

$$\left(\frac{T}{T_w}\right)^{0.8} - 0.8\left(\frac{T}{T_w}\right)^{0.8}\left(\frac{T_w}{T} - 1\right) + \frac{\cos\frac{\pi x}{L}}{\frac{YL}{K\pi}\frac{dT}{dx}} = 0 \tag{B11}$$

Substitution of equation (B9) into equation (B11) and use of the relation $\frac{dT}{dx} = \frac{K}{mgc_p}\sin\frac{\pi x}{L}$ (given by equations (5) and (B6)) result in

$$\left(\frac{T}{T_w}\right)^{0.8} = \frac{0.8\sin\frac{\pi x}{L}}{\frac{YT}{K}} - \frac{\cot\frac{\pi x}{L}}{\frac{YL}{mgc_p\pi}} \tag{B12}$$

From the definition of Y, let

$$\lambda = \frac{YL}{\pi mgc_p} = \frac{0.092}{\pi}\left(\frac{k_w}{c_{p,w}\mu_w}\right)^{0.6}\left(\frac{A\mu_{w,av}}{mgD_e}\right)^{0.2}\frac{L}{D_e} \tag{B13}$$

Note that $\frac{YT}{K} = \frac{\pi mgc_pT}{KL}\lambda$, which, from equations (B7) and (B8), gives

$$\frac{YT}{K} = \lambda\left[\frac{2}{\frac{T_{ex}}{T_{en}} - 1} + \left(1 - \cos\frac{\pi x}{L}\right)\right] \tag{B14}$$

Hence, equation (B12) may be written as

$$\left(\frac{T}{T_w}\right)^{0.8} = \frac{1}{\lambda}\left[\frac{0.8 \sin \frac{\pi x}{L}}{\frac{2}{\frac{T_{ex}}{T_{en}} - 1} + \left(1 - \cos \frac{\pi x}{L}\right)} - \cot \frac{\pi x}{L}\right] = \frac{\varphi}{\lambda} \tag{B15}$$

2100

where φ is a function of x/L and T_{ex}/T_{en} as defined by equation (B15).

Substitution of equations (B14) and (B15) in equation (B9) and solution for λ give

$$\lambda = \left\{1 + \frac{\sin \frac{\pi x}{L}}{\left[\frac{2}{\frac{T_{ex}}{T_{en}} - 1} + \left(1 - \cos \frac{\pi x}{L}\right)\right]\varphi}\right\}^{0.8} \varphi \tag{B16}$$

In equations (B15) and (B16), λ and φ are given as functions of the basic variables x/L and T_{ex}/T_{en}. From equation (B15), the corresponding value of T/T_w, which is given by $dT_w/dx = 0$ and hence is actually $T/T_{w,max}$, is determined. From equations (B7) and (B8), $T_{en}/T_{w,max}$ is then obtained. Note that for monatomic gases ($\gamma = 5/3$ and $c_p\mu/k = 2/3$ by equation (9)), $\lambda = 0.03736 \left(\frac{A\mu_{w,av}}{mgD_e}\right)^{0.2} \frac{L}{D_e}$ by equation (B13). A plot of $T_{en}/T_{w,max}$ against $\left(\frac{A\mu_{w,av}}{mgD_e}\right)^{0.2} \frac{L}{D_e}$ for various values of T_{ex}/T_{en} is presented as figure 6.

REFERENCES

1. Nielsen, Jack N.: High-Altitude Cooling. III - Radiators. NACA ARR L4I11b, 1944.

2. Becker, John V., and Baals, Donald D.: Simple Curves for Determining the Effects of Compressibility on Pressure Drop through Radiators. NACA ACR L4I23, 1944.

3. Valerino, Michael F.: Generalized Charts for Determination of Pressure Drop of a High-Speed Compressible Fluid in Heat-Exchanger Passages. I - Air Heated in Smooth Passages of Constant Area with Constant Wall Temperature. NACA RM E8G23, 1948.

4. Sibulkin, Merwin, and Koffel, William K.: Chart for Simplifying Calculations of Pressure Drop of a High-Speed Compressible Fluid under Simultaneous Action of Friction and Heat Transfer - Application to Combustion-Chamber Cooling Passages. NACA TN 2067, 1950.

5. Pinkel, Benjamin, Noyes, Robert N., and Valerino, Michael F.: Method for Determining Pressure Drop of Air Flowing through Constant-Area Passages for Arbitrary Heat-Input Distributions. NACA TN 2186, 1950.

6. Humble, Leroy V., Lowdermilk, Warren H., and Grele, Milton: Heat Transfer from High-Temperature Surfaces to Fluids. I - Preliminary Investigation with Air in Inconel Tube with Rounded Entrance, Inside Diameter of 0.4 Inch, and Length of 24 Inches. NACA RM E7L31, 1948.

7. Lowdermilk, Warren H., and Grele, Milton D.: Heat Transfer from High-Temperature Surfaces to Fluids. II - Correlation of Heat-Transfer and Friction Data for Air Flowing in Inconel Tube with Rounded Entrance. NACA RM E8L03, 1949.

8. Desmon, Leland G., and Sams, Eldon W.: Correlation of Forced-Convection Heat-Transfer Data for Air Flowing in Smooth Platinum Tube with Long-Approach Entrance at High Surface and Inlet-Air Temperatures. NACA RM E50H23, 1950.

9. Turner, L. Richard, Addie, Albert N., and Zimmerman, Richard H.: Charts for the Analysis of One-Dimensional Steady Compressible Flow. NACA TN 1419, 1948.

10. Keesom, W. H.: Helium. Univ. of Leiden (Amsterdam), 1942, p. 107.

2100

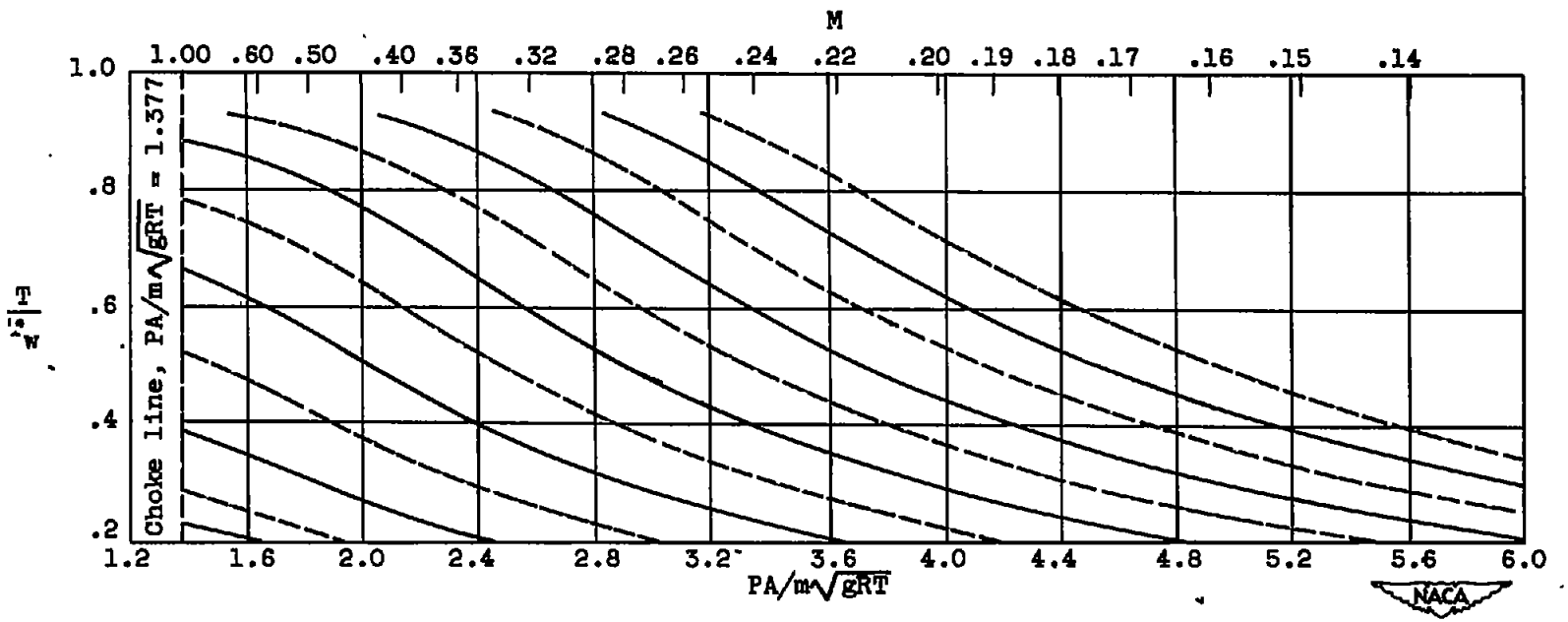

Figure 1. - Variation of total-pressure parameter with ratio of fluid total temperature to passage-wall temperature. Turbulent flow of monatomic gases ($\gamma = 5/3$) through smooth passages with constant wall temperature. (A 22- by $8\frac{1}{2}$-in. print of this fig. is attached.)

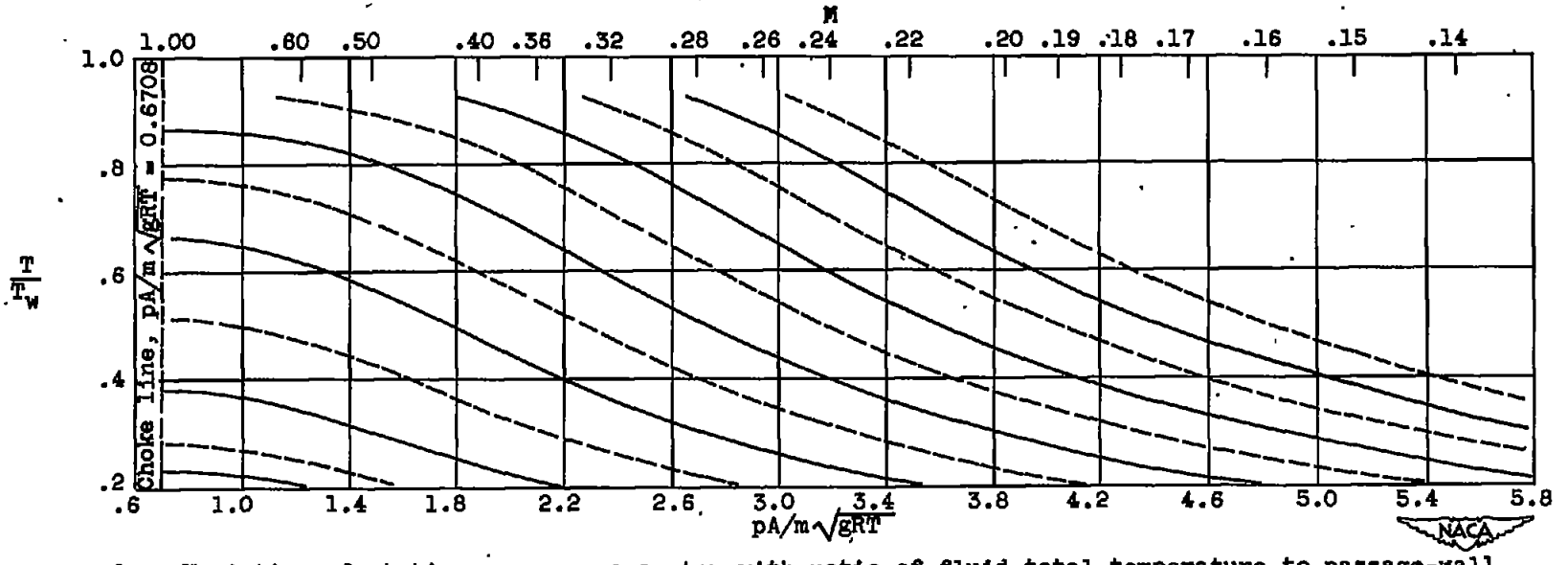

Figure 2. - Variation of static-pressure parameter with ratio of fluid total temperature to passage-wall temperature. Turbulent flow of monatomic gases ($\gamma = 5/3$) through smooth passages with constant wall temperature. (A 22- by 8-in. print of this fig. is attached.)

2100

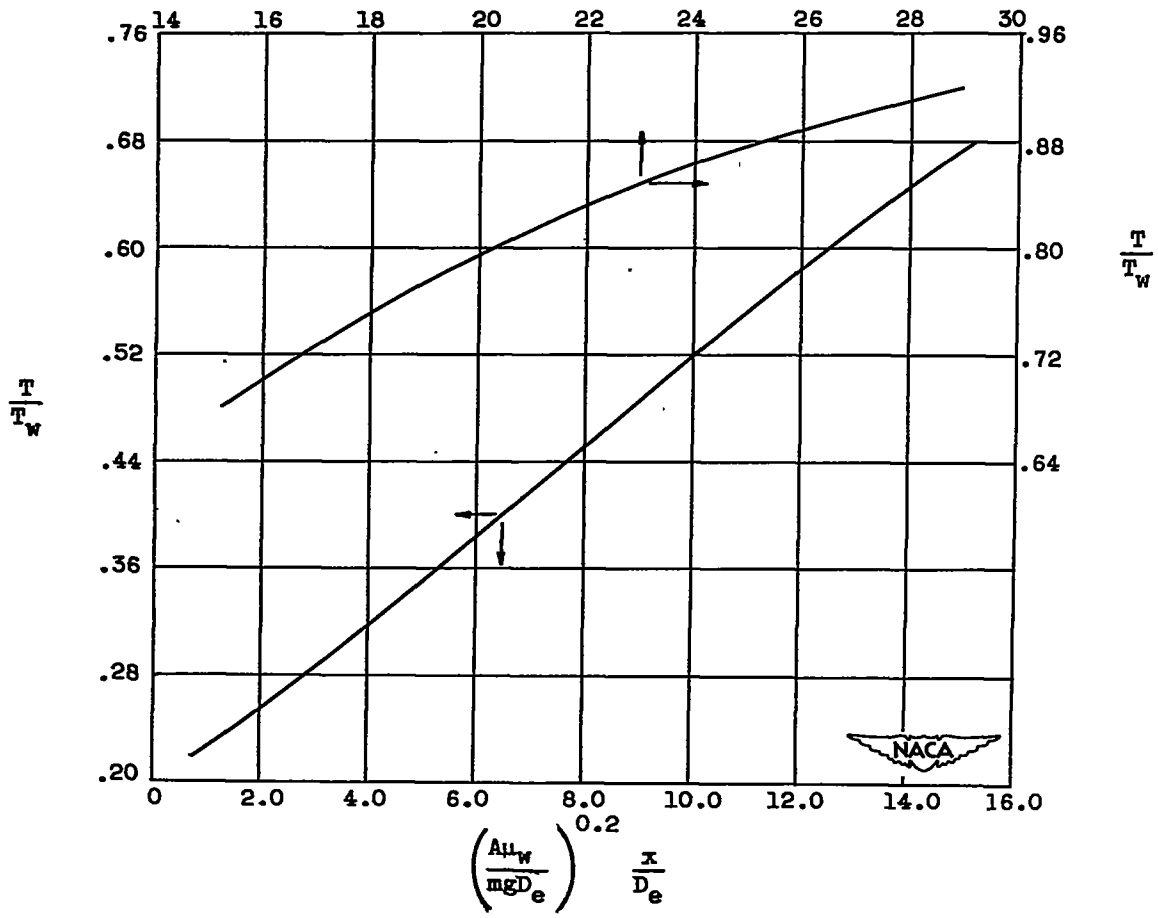

Figure 3. - Variation of ratio of fluid to wall temperature with distance parameter for monatomic gases ($\gamma = 5/3$) and constant wall-temperature conditions. (A 19- by 17-in. print of this fig. is attached.)

2100

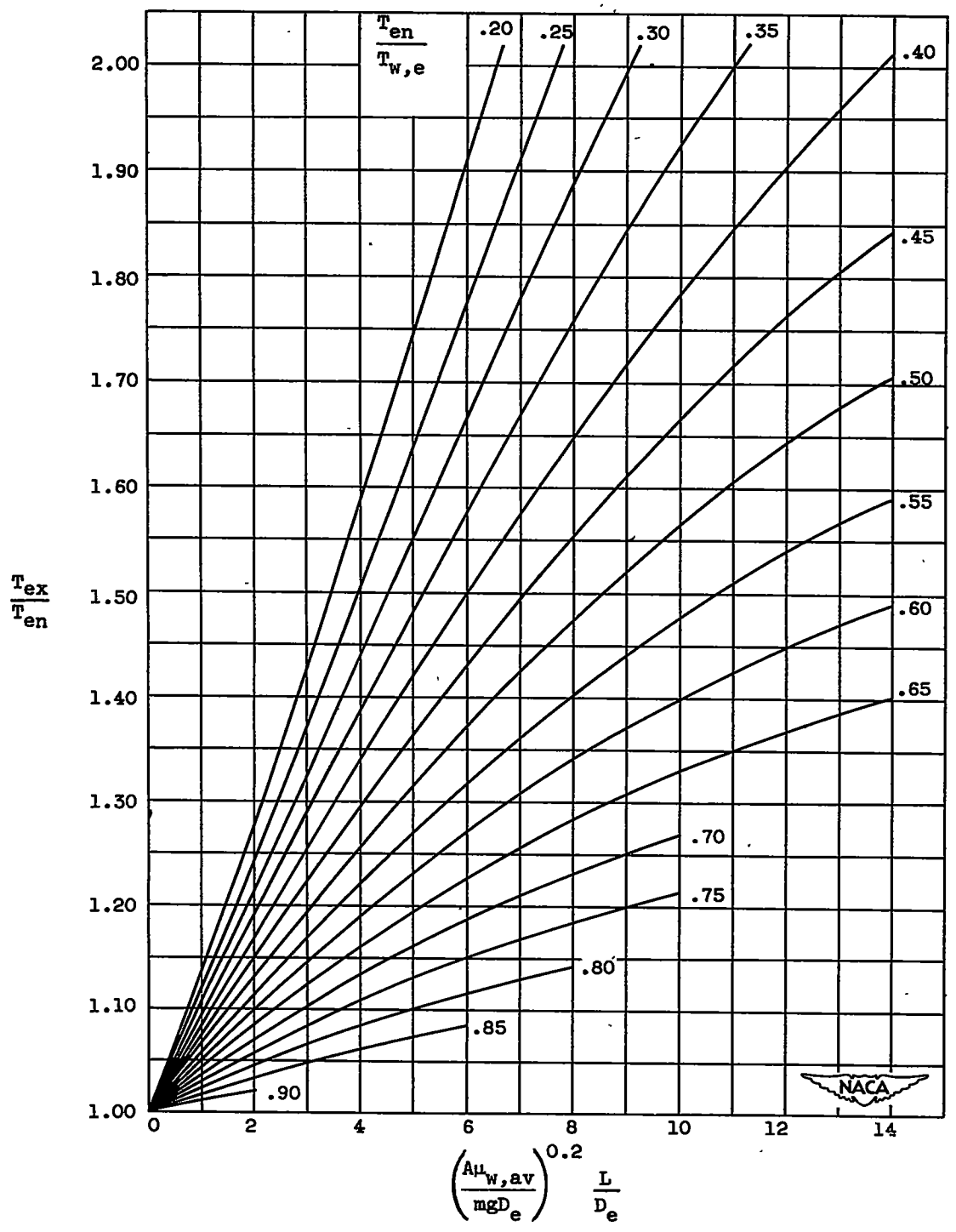

(a) Ratio of exit to entrance fluid temperature, 1.0 to 2.02.

Figure 4. - Chart for determination of effective constant wall temperature that results in any given fluid-temperature rise within flow passage. Turbulent flow of monatomic gases ($\gamma = 5/3$). (A 15- by 21-in. print of this fig. is attached.)

2100

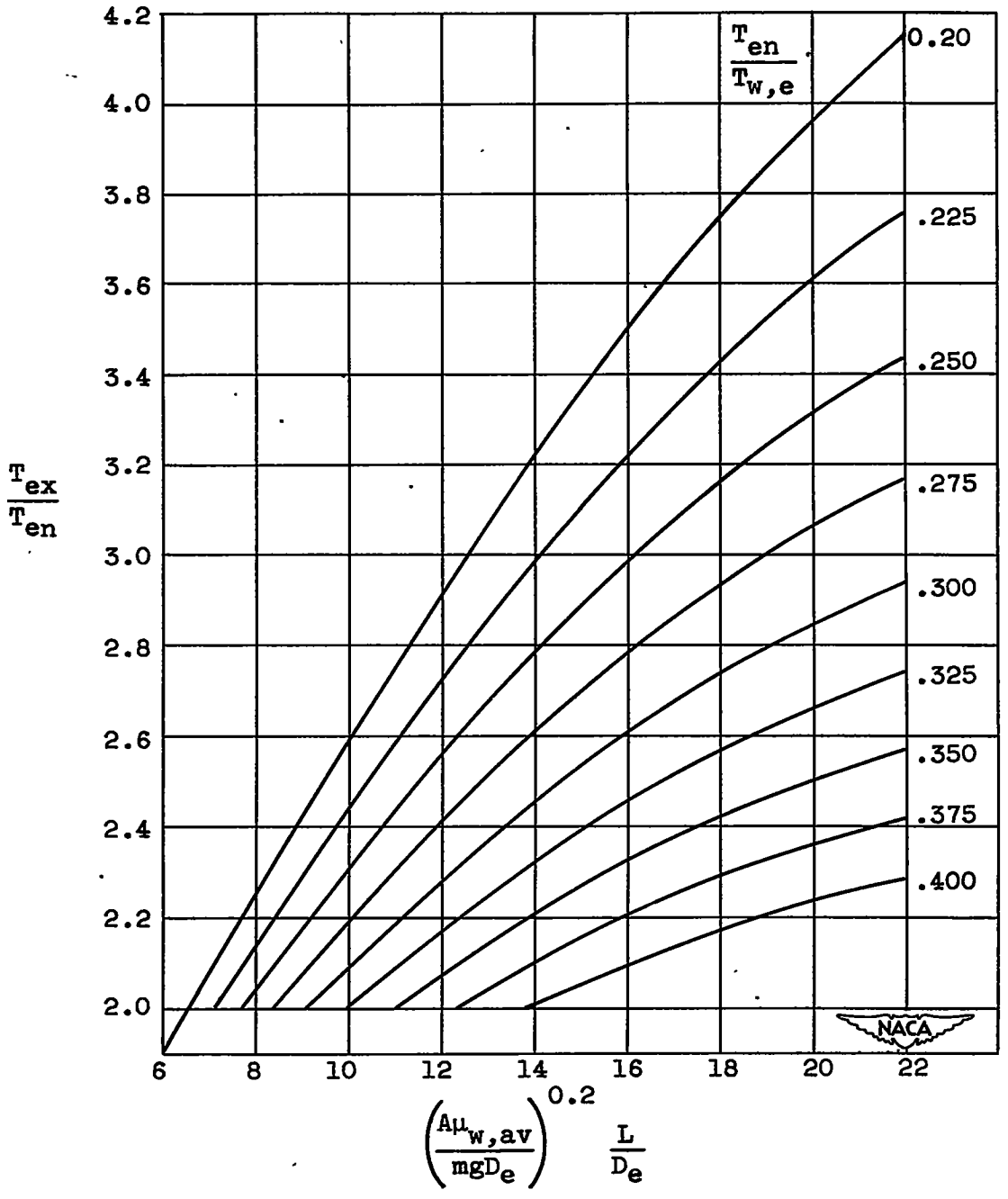

(b) Ratio of exit to entrance fluid temperature, 2.00 to 4.15.

Figure 4. - Concluded. Chart for determination of effective constant wall temperature that results in any given fluid-temperature rise within flow passage. Turbulent flow of monatomic gases ($\gamma = 5/3$). (A 11- by 15-in. print of this fig. is attached.)

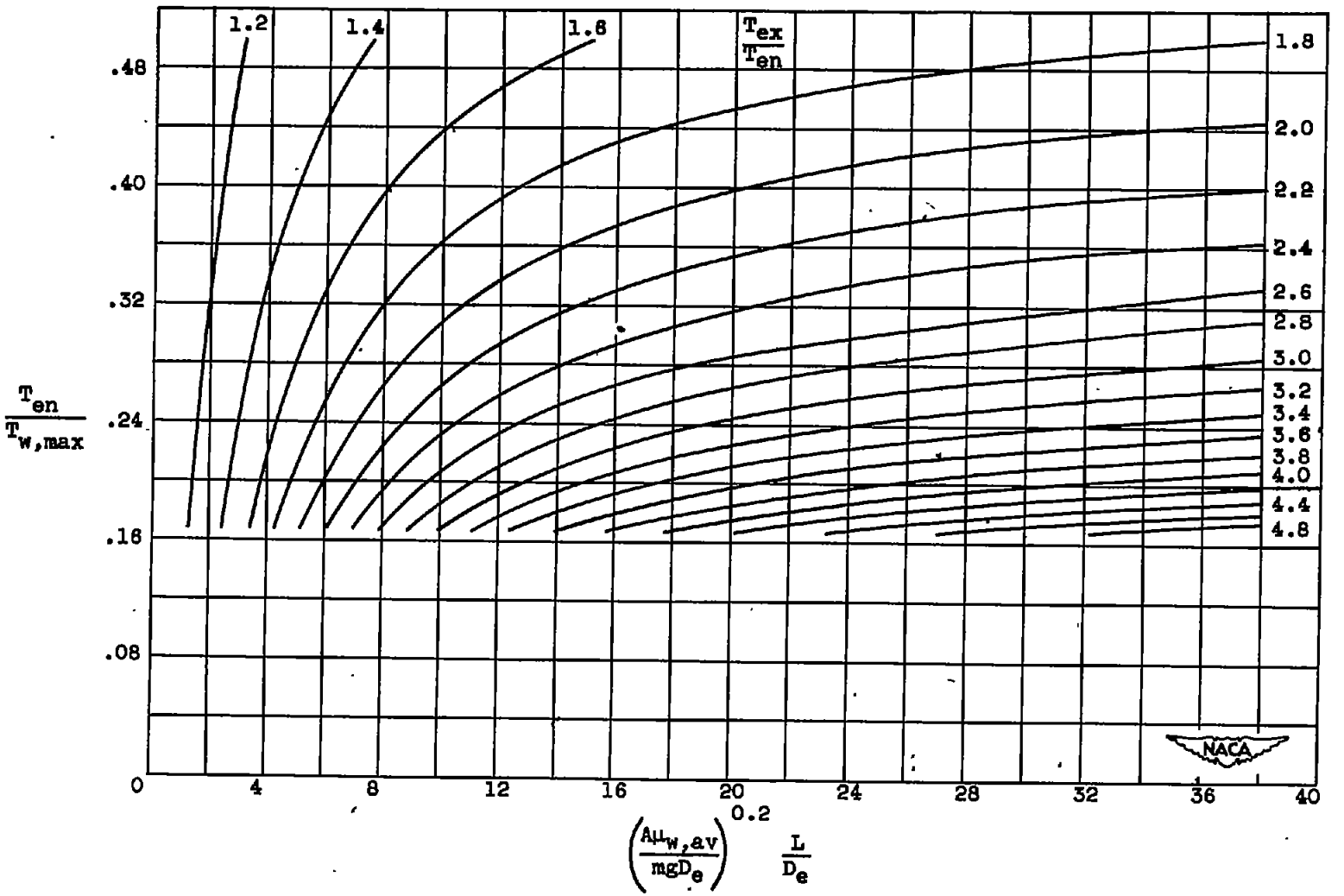

Figure 5. - Variation of ratio of fluid-entrance temperature to maximum passage-wall temperature with passage-length parameter and fluid-temperature ratio. Turbulent flow of monatomic gases ($\gamma = 5/3$) for conditions of constant rate of heat input. (A 22- by 16- in. print of this fig. is attached.)

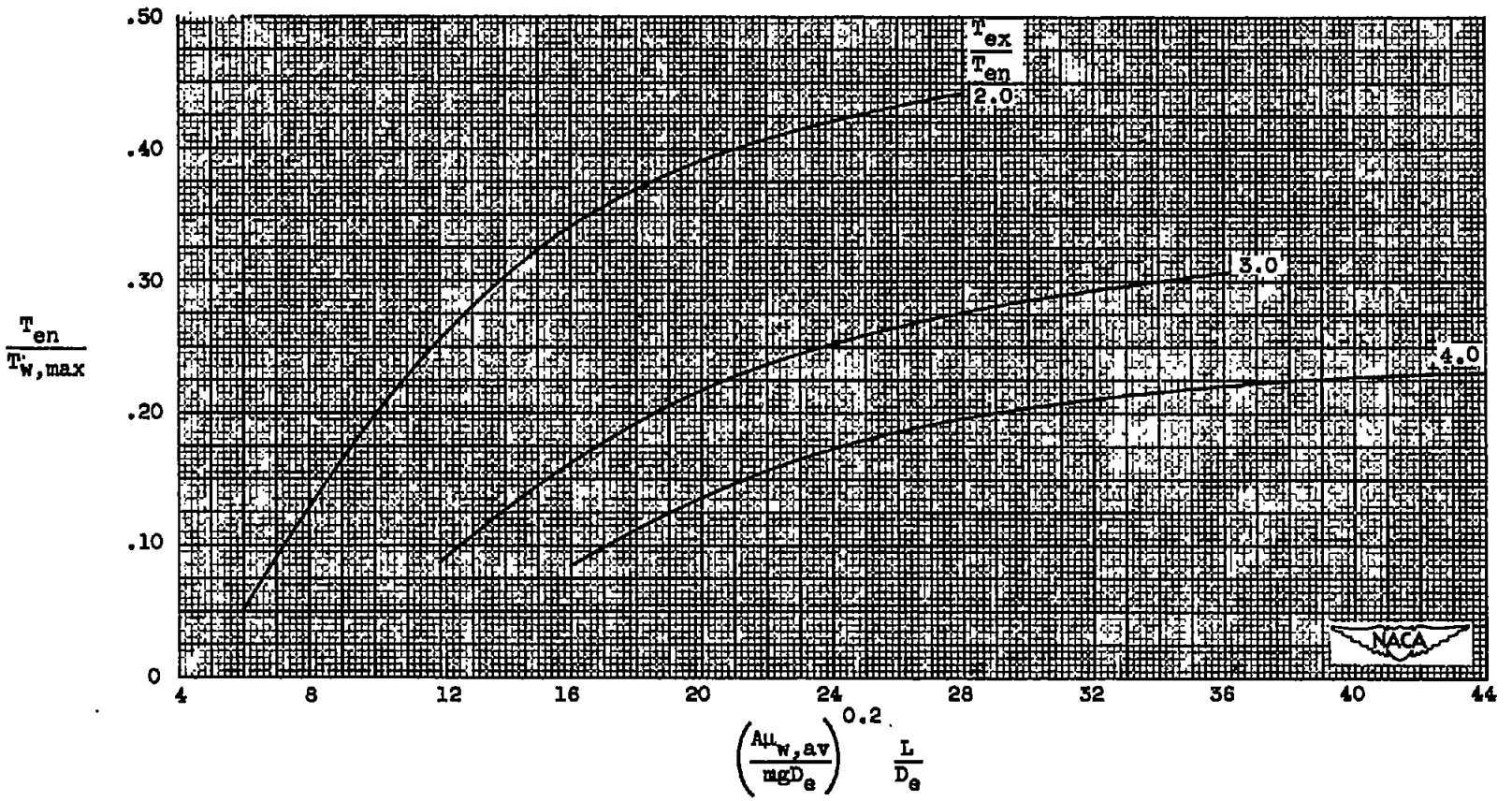

Figure 6. - Variation of ratio of fluid-entrance temperature to maximum passage-wall temperature with passage-length parameter and fluid-temperature ratio for sine variation of heat input to fluid.

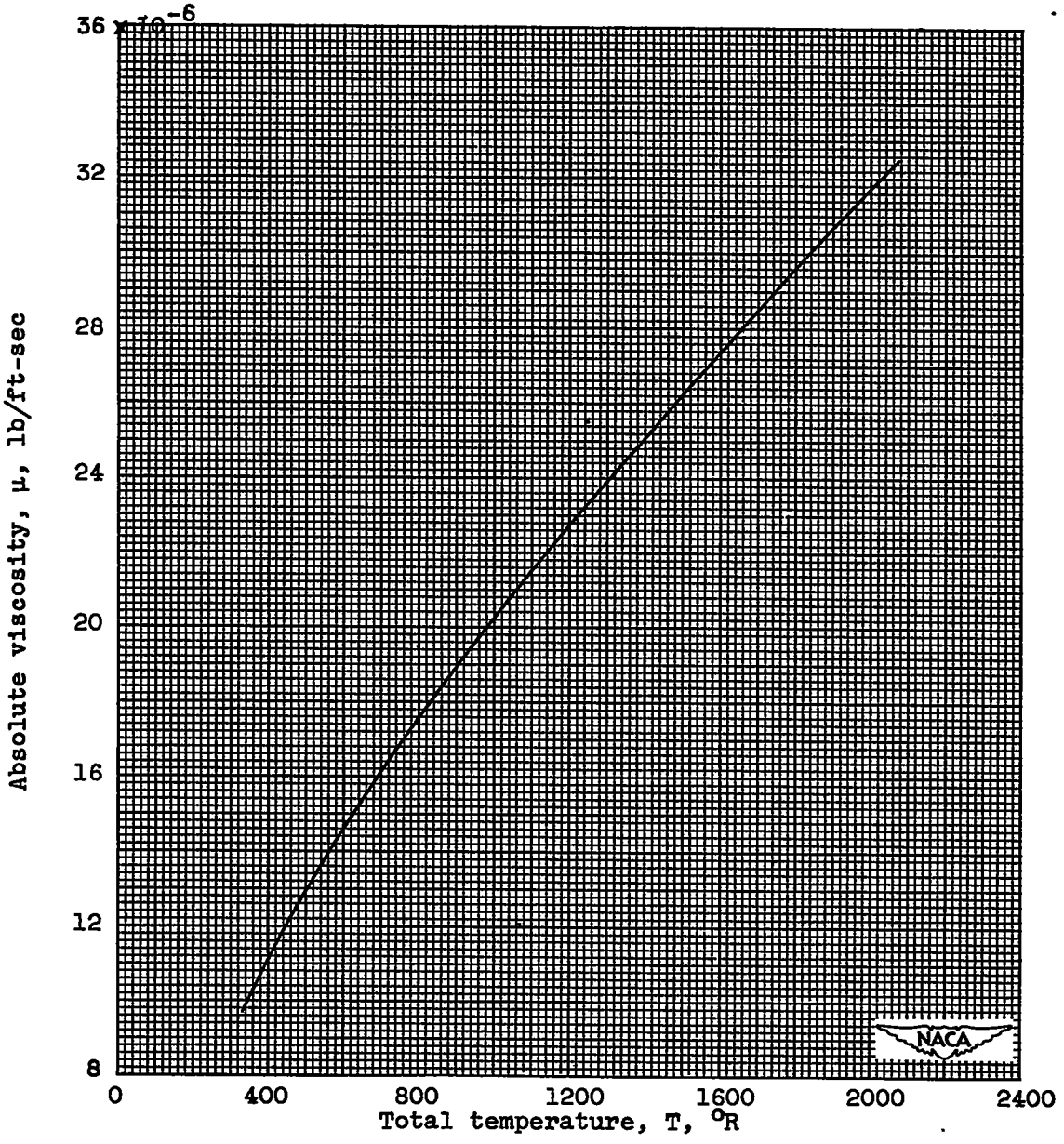

Figure 7. - Variation of absolute viscosity of helium with temperature.

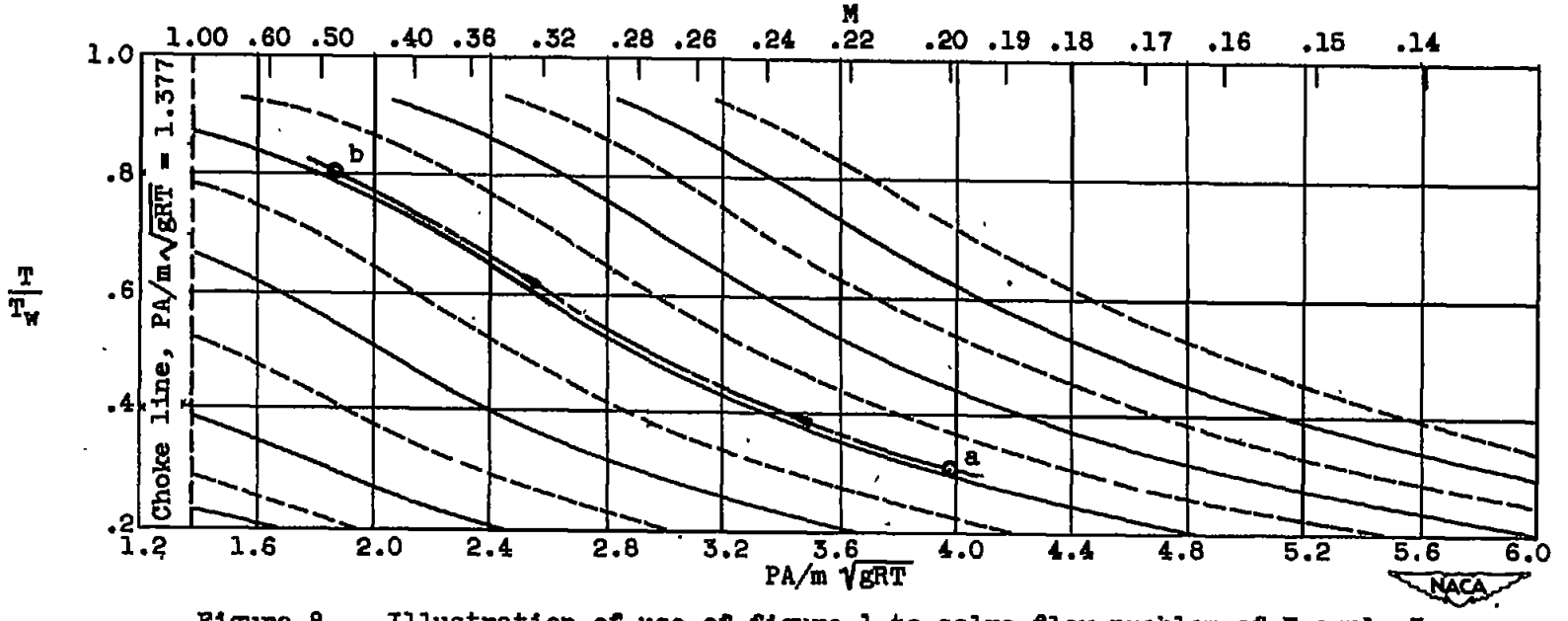

Figure 8. - Illustration of use of figure 1 to solve flow problem of Example I.

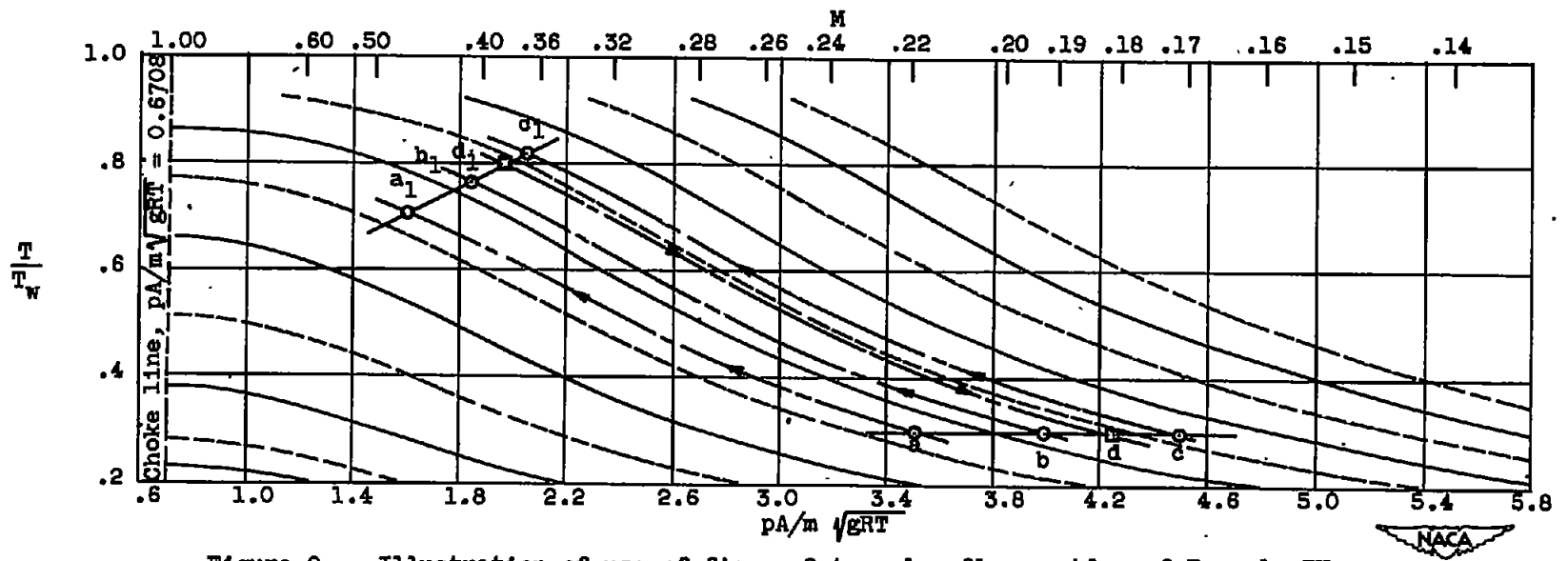

Figure 9. - Illustration of use of figure 2 to solve flow problem of Example IV.

NACA-Langley - 4-19-51 - 1100

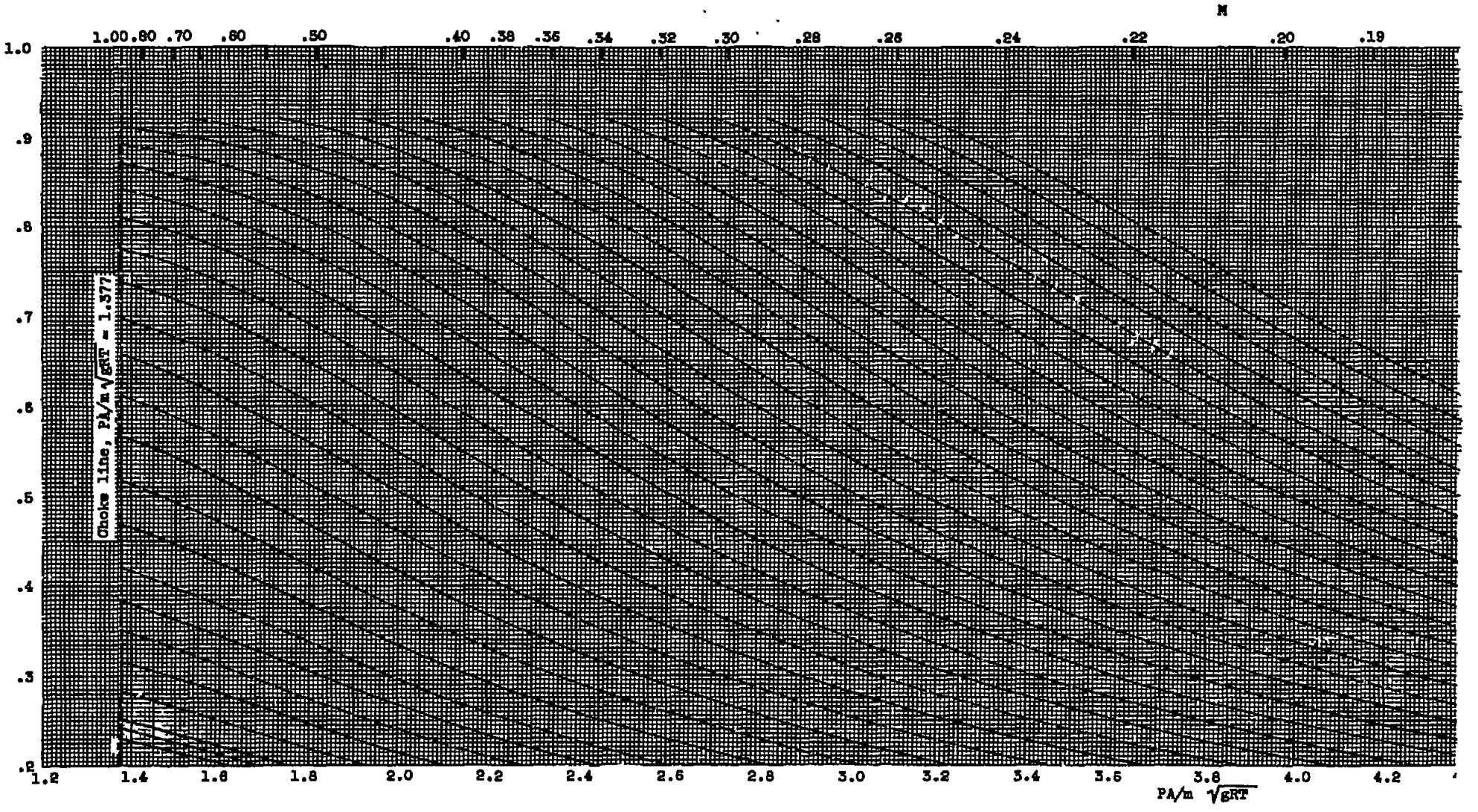

NACA-Langley - 4-16-51 - 1100

Figure 1. - Variation of total-pressure parameter with ratio of fluid total temperature to passage-wall temperature. Turbulent flow of m

[redacted]

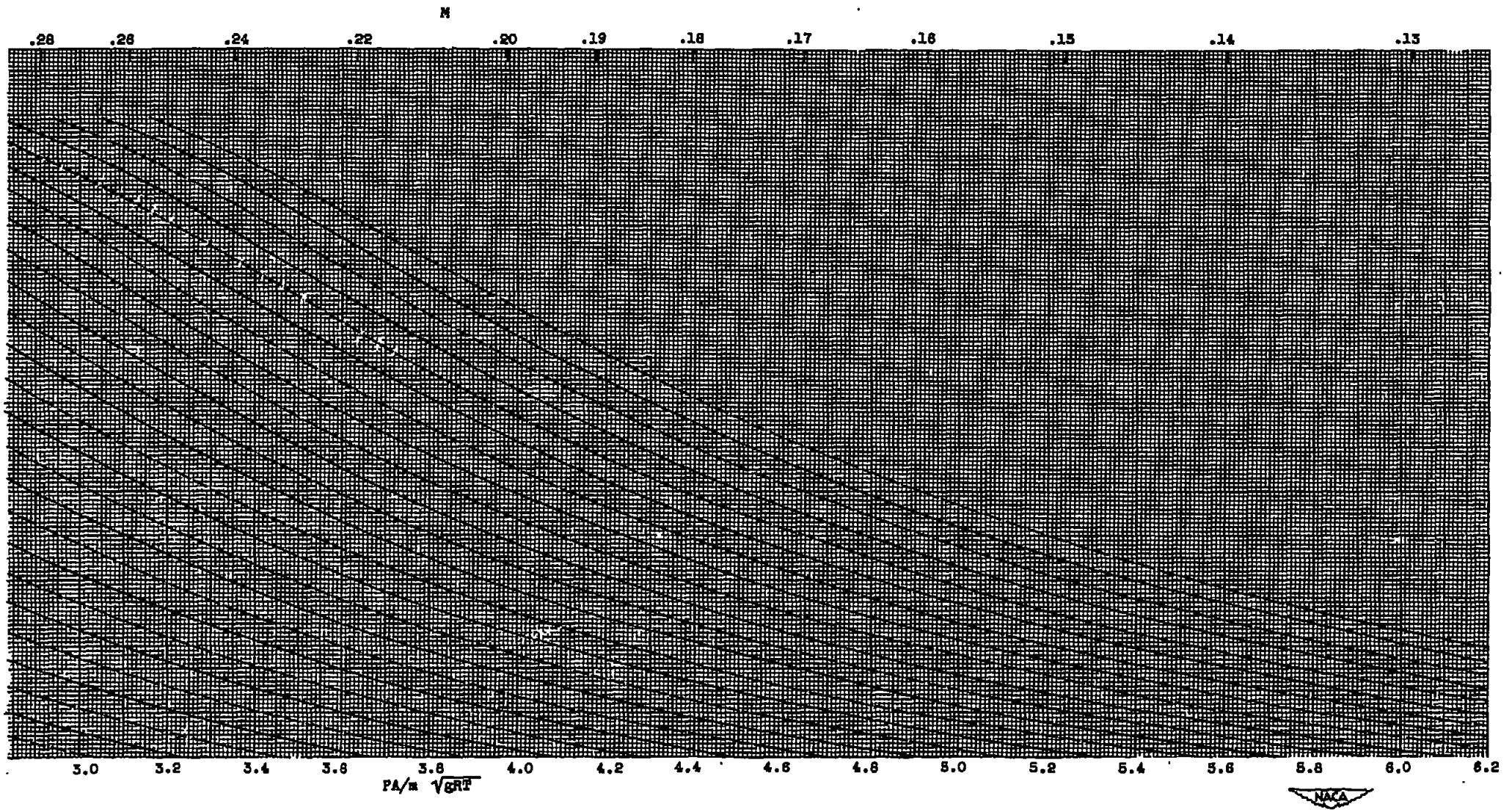

of fluid total temperature to passage-wall temperature. Turbulent flow of monatomic gases ($\gamma = 5/3$) through smooth passages with constant wall temperature.

[redacted]

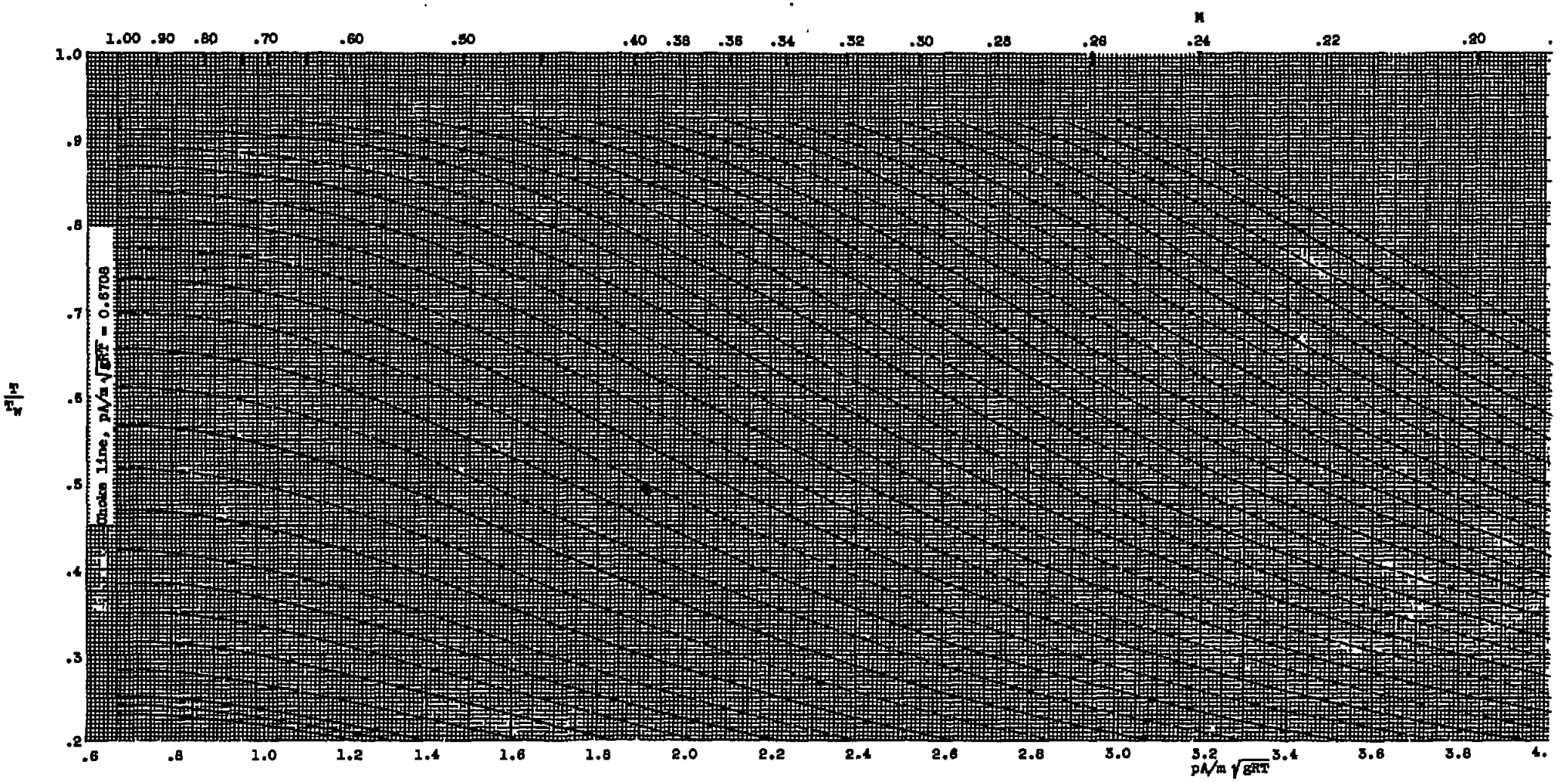

NACA-Langley - 4-17-51 - 1100

Figure 2. - Variation of static-pressure parameter with ratio of fluid total temperature to passage-wall temperature. Turbulent flow of monato

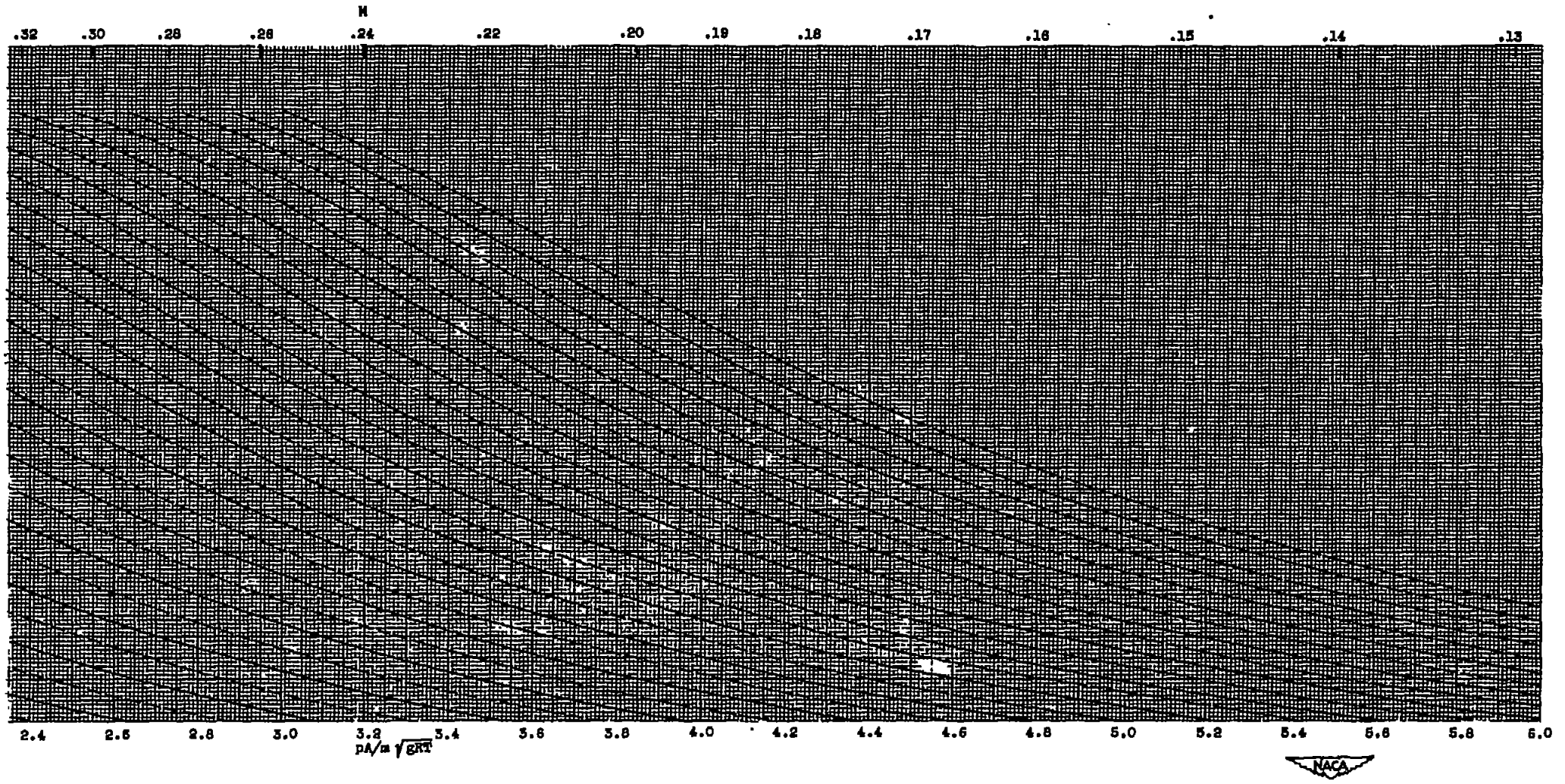

of fluid total temperature to passage-wall temperature. Turbulent flow of monatomic gases ($\gamma = 5/3$) through smooth passages with constant wall temperature.

2100

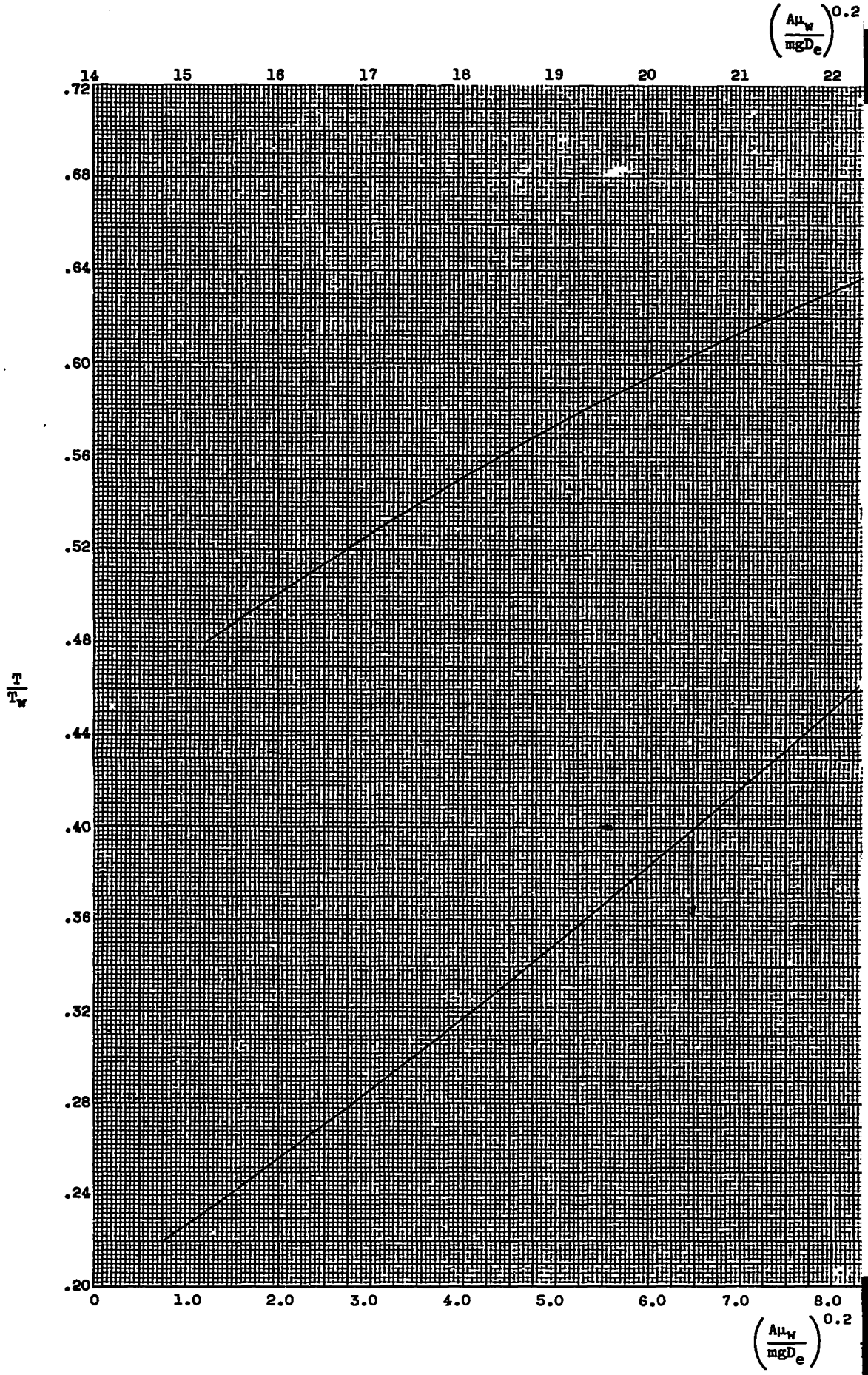

Figure 3. - Variation of ratio of fluid to wall temperature with distance parameter

NACA-Langley - 4-17-61 - 1100

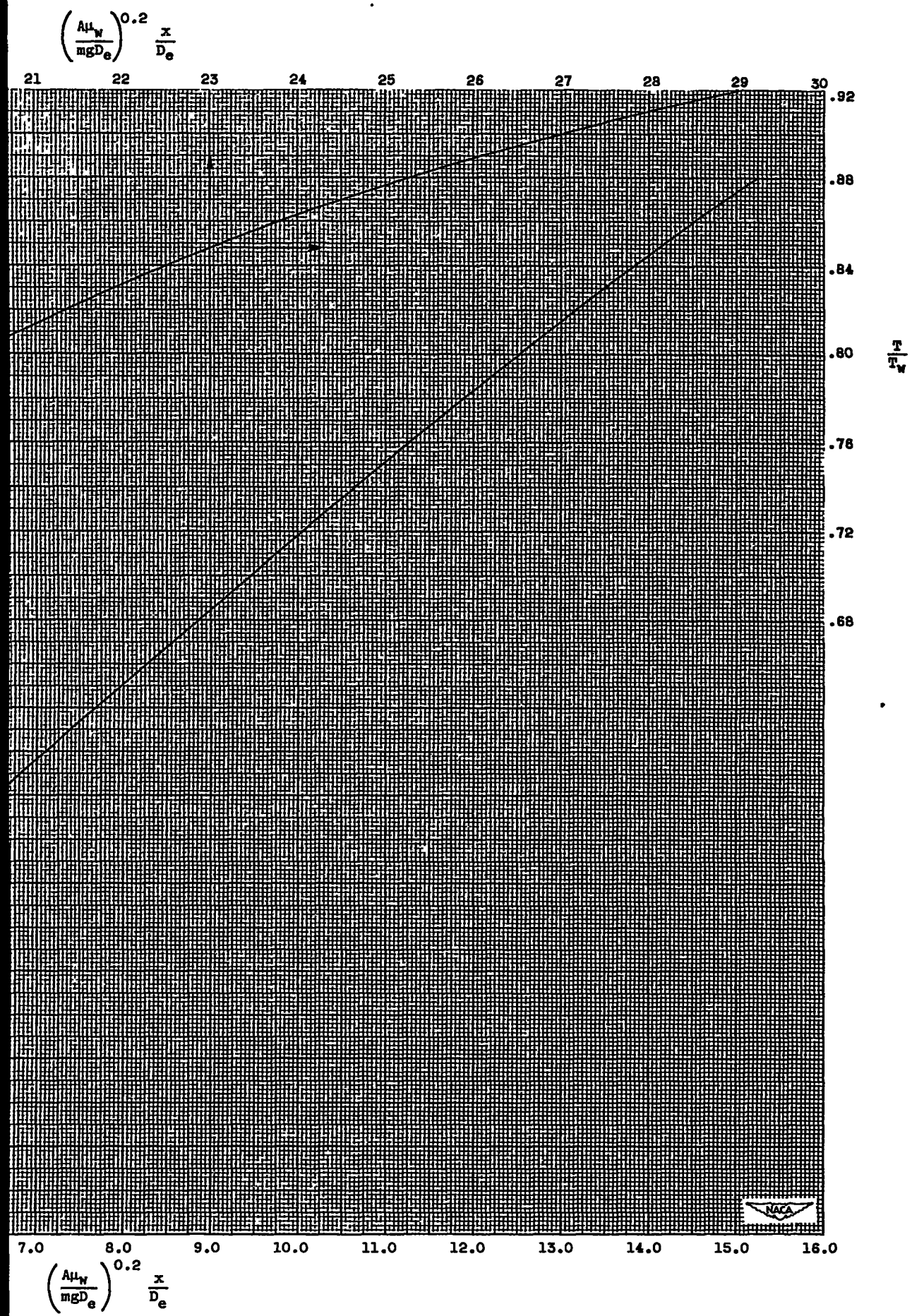

stance parameter for monatomic gases ($\gamma = 5/3$) and constant wall-temperature conditions.

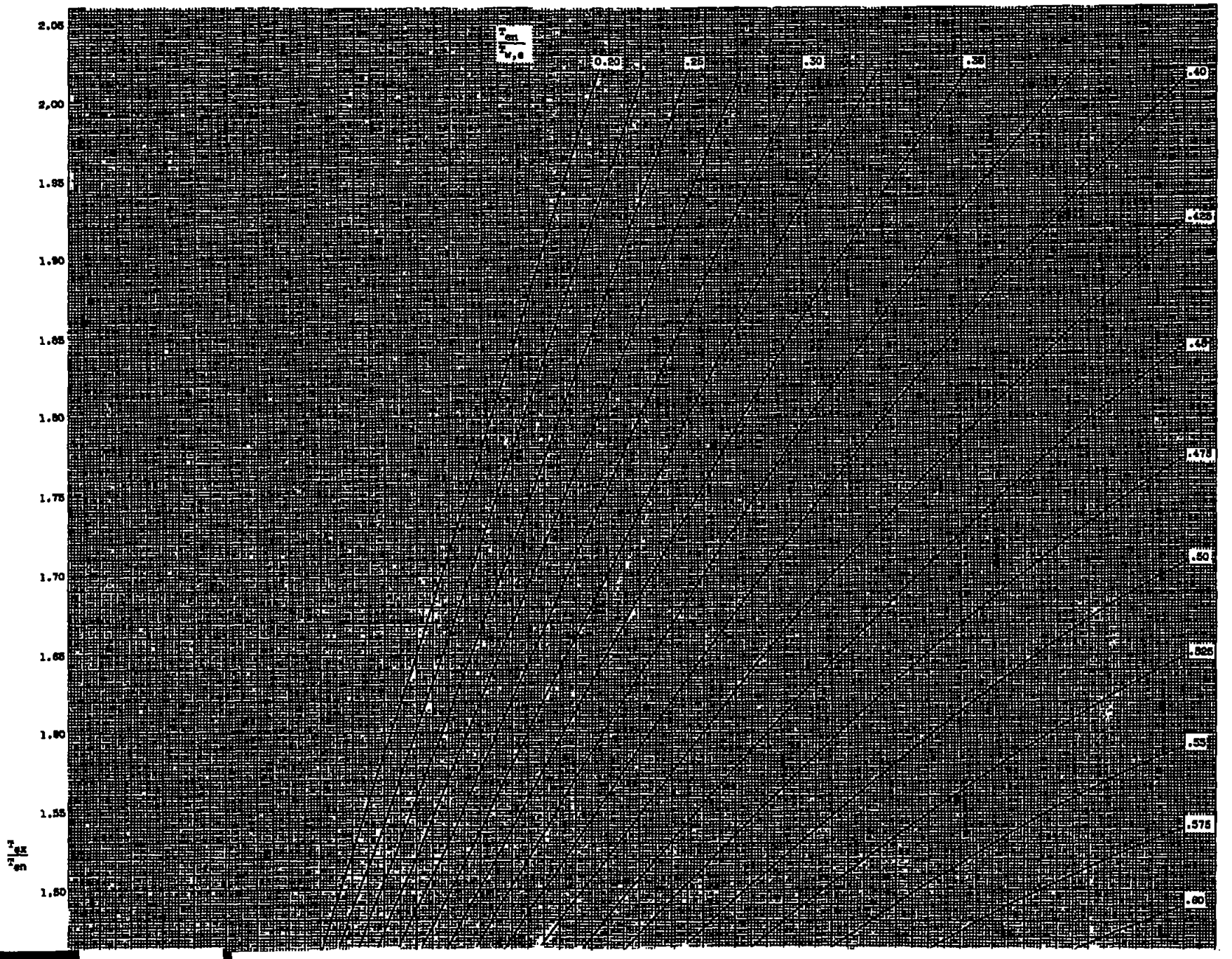
$\frac{\tau_{em}}{\tau_{w,e}}$
0.20
.25
.30
.35
.40
.425
.45
.475
.50
.525
.55
.575
.60
2.05
2.00
1.95
1.90
1.85
1.80
1.75
1.70
1.65
1.60
1.55
1.50
$\frac{\tau_{ex}}{\tau_{en}}$

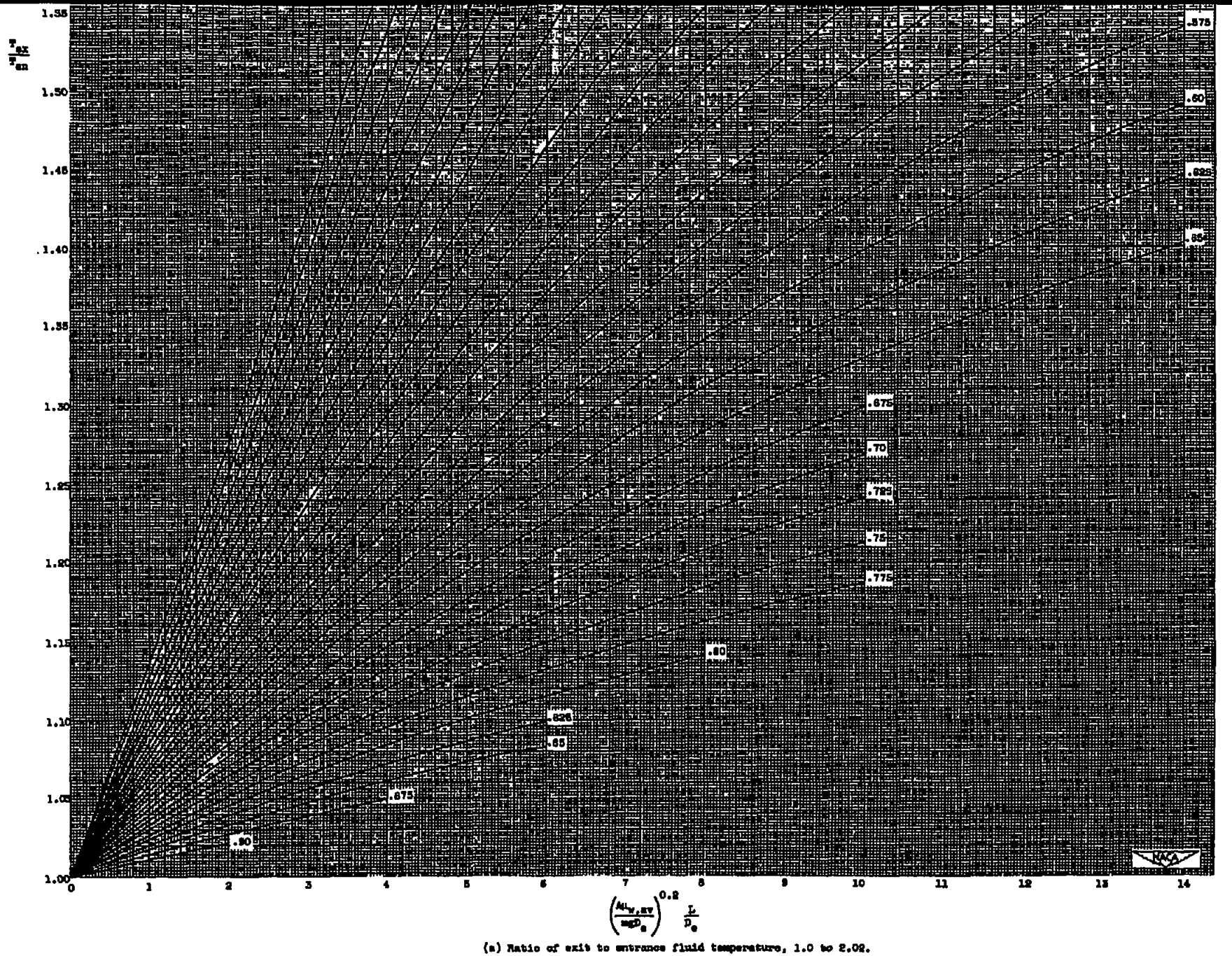

(a) Ratio of exit to entrance fluid temperature, 1.0 to 2.02.

Figure 4. - Chart for determination of effective constant wall temperature that results in any given fluid-temperature rise within flow passage. Turbulent flow of monatomic gases ($\gamma = 5/3$).

NACA-Langley - 4-19-51 - 1199

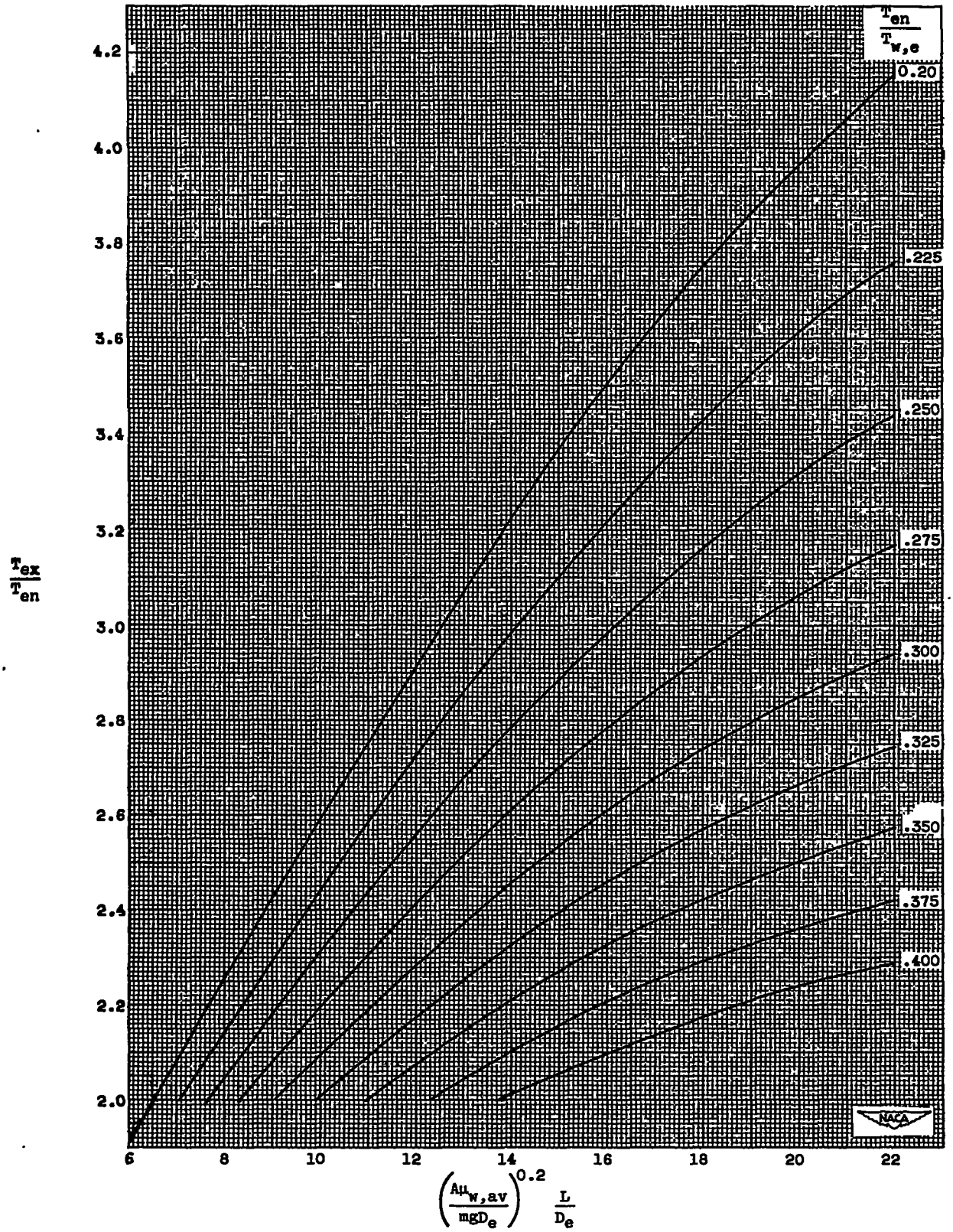

(b) Ratio of exit to entrance fluid temperature, 2.00 to 4.15.

Figure 4. - Concluded. Chart for determination of effective constant wall temperature that results in any given fluid-temperature rise within flow passage. Turbulent flow of monatomic gases ($\gamma = 5/3$).

NACA-Langley - 4-17-51 - 1100

2100

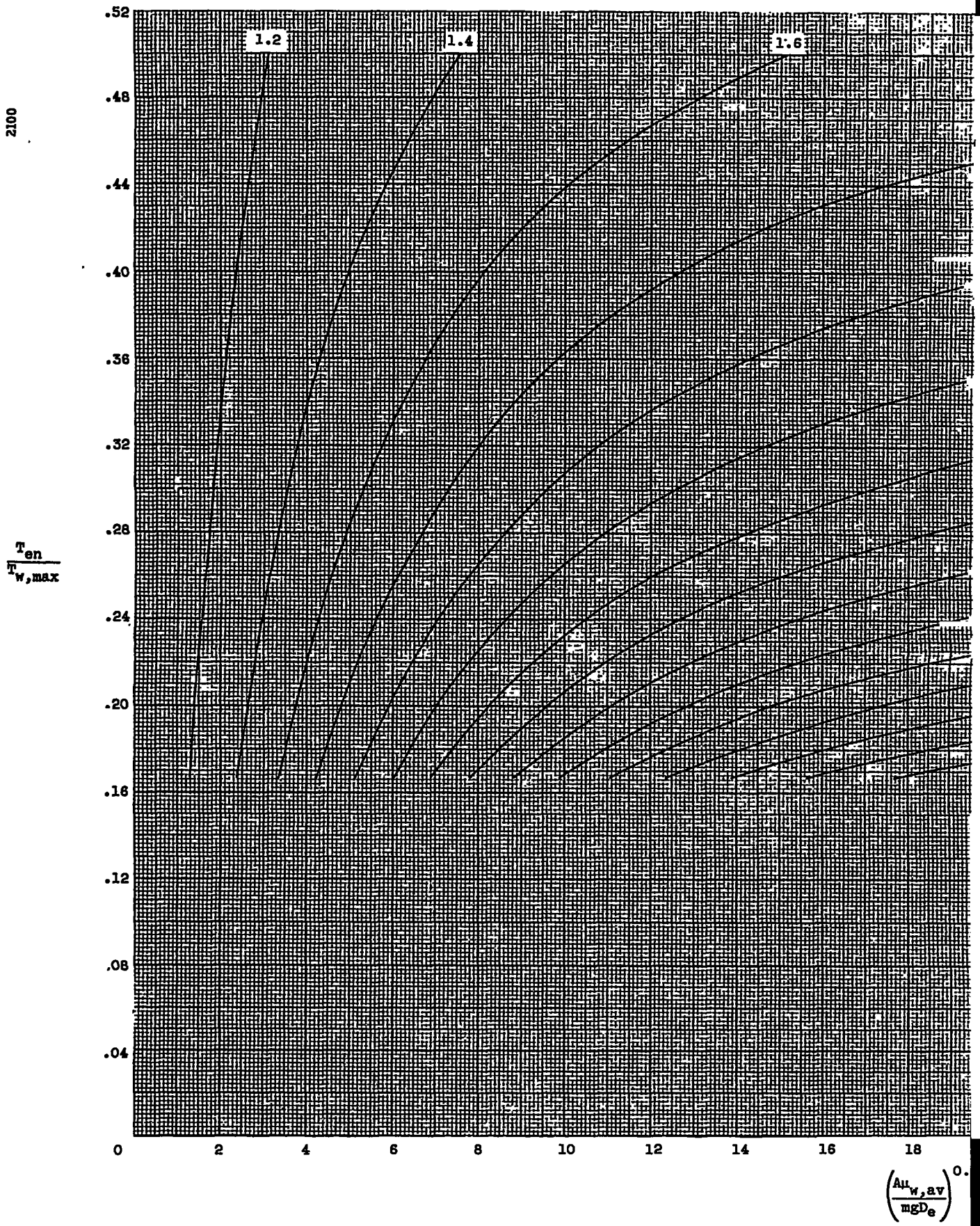

Figure 5. - Variation of ratio of fluid-entrance temperature to maximum passage-wall temperature with passage
conditions of constant r

NACA-Langley - 4-16-51 - 1100

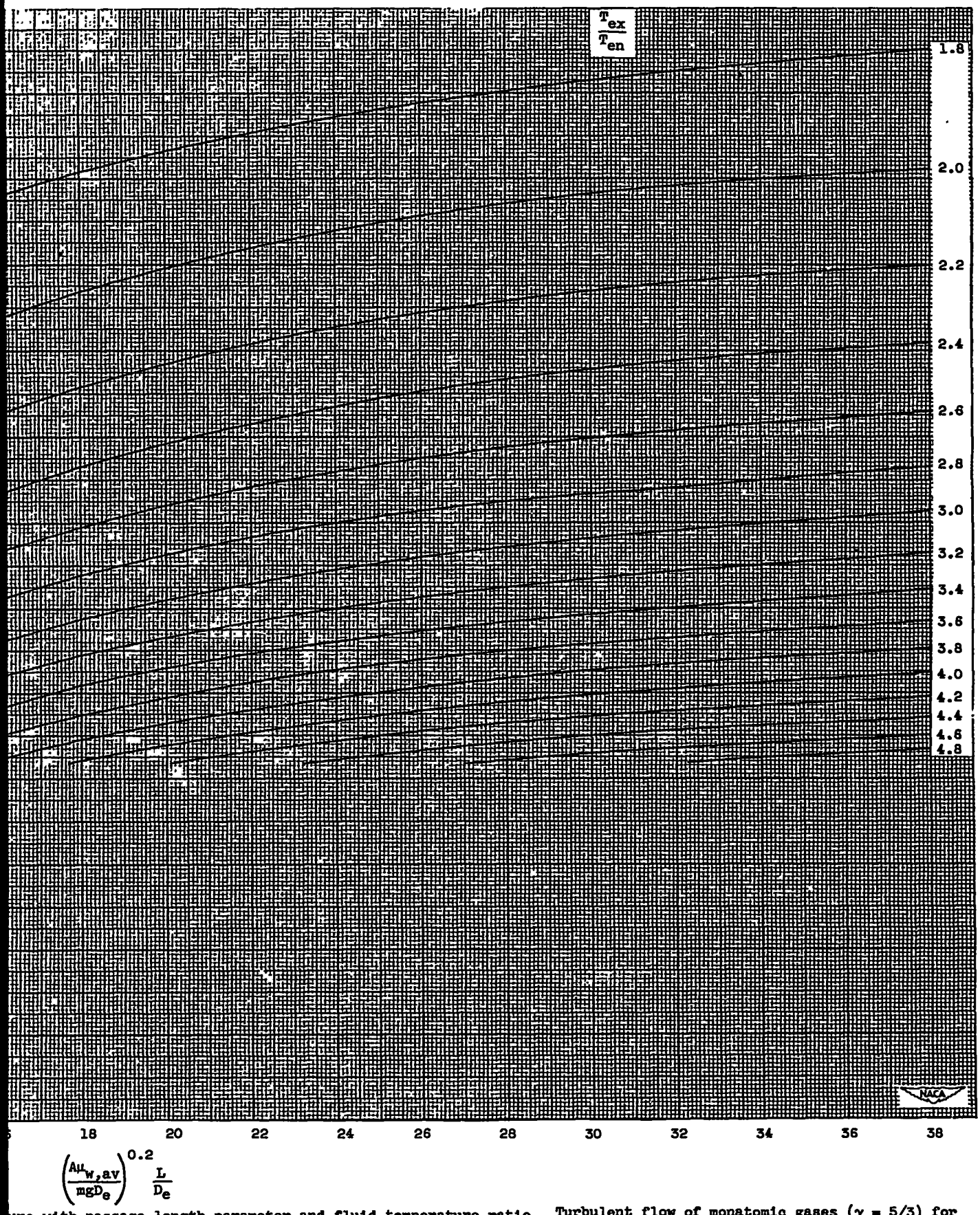

ure with passage-length parameter and fluid-temperature ratio. Turbulent flow of monatomic gases ($\gamma = 5/3$) for ns of constant rate of heat input.